ANALYSIS OF FLUTTER AND FLUTTER SUPPRESSION VIA AN ENERGY METHOD

by

Darrell L. York

Thesis submitted to the Graduate Faculty of the

Virginia Polytechnic Institute and State University

in partial fulfillment of the requirements for the degree of

MASTER OF SCIENCE

in

Aerospace and Ocean Engineering

APPROVED:

Dr. E. M. Cliff, Chairman

Dr. F. H. Lutze

Dr. T. A. Weisshaar

May, 1980

Blacksburg, Virginia

ACKNOWLEDGMENTS

Special thanks are due to Dr. Eugene M. Cliff who was the principal advisor for this thesis and whose encouragement, patience, and breadth of knowledge made this study possible. Thanks are also due to Dr. F. H. Lutze and Dr. T. A. Weisshaar for their advice and careful review of this work.

TABLE OF CONTENTS

LIST OF TABLES

LIST OF FIGURES

Figure Page

NOMENCLATURE

A	dimensional system matrix
A_i	aerodynamic state variables; subscript indicates correspondence with ith term in exponential approximation to the Wagner function
A_j	magnitude of aerodynamic forces and motion variables
A_{ii}	submatrix of system matrix
A_{T_s}	magnitude of servo torque
a	arbitrary feedback matrix element used in eq. 5.29
B_i	aerodynamic state variables; subscript indicates correspondence with ith term in exponential approximation to the Wagner function
b	semichord; control matrix
$C(k)$	Theodorsen function
c	nondimensionalized distance of flap hinge line from e.a.
$D(t)$	Duhamel integral of $Q_1'(t)$ and Wagner function
d	nondimensionalized distance of e.a. from leading edge
$\dot{E}$	time rate of change of Kinetic energy
$\dot{E}_{aero}$	rate at which Kinetic energy is being transferred from the surrounding airstream to the airfoil
$\dot{E}_{control}$	servo torque contribution to rate of Kinetic energy transfer
$\dot{E}_{no}$	Kinetic energy rate for non-oscillatory modes
$\dot{E}_{spring}$	rate of Kinetic energy transfer due to spring forces
$\dot{E}_{total}$	total instantaneous Kinetic energy rate
ΔE	change in Kinetic energy per cycle defined in eq. 7.1
e	subspace orthogonal to Z
e_i	elements of e

$e^{\perp}$	subspace orthogonal to e
f	feedback row matrix
$\vec{F}$	resultant force
F_s	constraint force for mass-spring system
G(t)	Duhamel integral of $Q_2'(t)$ and Wagner function
$\mathcal{F}$	Fourier transform operator $\mathcal{F} f(t) = \int_{-\infty}^{+\infty} f(t)\exp(-i\omega t)dt$
H	constraint vector associated with the Kinematic control law
h	vertical deflection of e.a., positive down
I_Q, I_β	moments of inertia per unit length of total section, and trailing edge flap about x_1 and c respectively
I_G	moment of inertia per unit span of trailing-edge flap about pt. G
I_α	moment of inertia per unit length of main section about x_α
i	$\sqrt{-1}$
$\vec{j}$	unit vector
K	stiffness matrix
$k_{1,2}$	spring stiffnesses for mass-spring system
K'	unsymmetrical form of stiffness matrix
K_h	stiffness of wing in vertical deflection
K_α	torsional stiffness of wing about e.a.
K_β	torsional stiffness of trailing edge flap about c
k	reduced frequency ($=\omega b/V$)
L	lift per unit span
L_1	lift per unit span on main section of airfoil

L_2	lift per unit span on trailing-edge flap
$L_{\ddot{h}}, L_{\ddot{\alpha}}, L_{\ddot{\beta}}$	contributions to total lift defined in Appendix D
$L_{\dot{h}}, L_{\dot{\alpha}}, L_{\dot{\beta}}$	
$L_{\alpha}, L_{\beta}, L_{B_1}, L_{B_2}$	
ℓ	distance of trailing-edge flap center of gravity from c(ft.); coefficient in eq. 5.10
l	control law
l_i	control law component
Δl_i	small perturbation of the control law component
$\hat{l}_i$	initial value of the control law component
M	pitching moment per unit span about one-quarter chord; mass matrix
M_1	pitching moment per unit span of main section about one-quarter chord
M_2	pitching moment per unit span of trailing-edge flap about c
M'	unsymmetrical form of mass matrix
$M_{e.a.}$	pitching moment per unit span about elastic axis
$M_{\ddot{h}}, M_{\ddot{\alpha}}, M_{\ddot{\beta}}$	contributions to total one-quarter chord pitching moment
$M_{\dot{\alpha}}, M_{\dot{\beta}}, M_{\beta}$	defined in Appendix D
m	mass of airfoil per unit length
m_1	mass of main section per unit length; mass of body 1 in mass-spring system
m_2	mass of trailing-edge flap per unit length; mass of body 2 in mass-spring system
n	coefficient in eq. 5.10; dimension of basis for $V^{\perp}$

$Q_1'(t)$, $Q_2'(t)$	expressions defined in (B. 16) and (B. 17)
P	quantity defined in eq. 5.17; matrix that projects vectors along $V^{\perp}$ onto V
P_l	pressure on lower surface of airfoil element
P_u	pressure on upper surface of airfoil element
q_y	vertical flap hinge force
S_α	static moment of airfoil per unit length about x_α
S_β	static moment of trailing-edge flap per unit length about c
T	flap aerodynamic hinge moment per unit span
T_s	servo torque per unit span of trailing-edge flap about c
$T_{\ddot{h}}, T_{\ddot{\alpha}}, T_{\ddot{\beta}}$	contributions to aerodynamic hinge moment defined in Appendix D
$T_{\dot{h}}, T_{\dot{\alpha}}, T_{\dot{\beta}}$	
$T_\alpha, T_\beta, T_{A_1}, T_{A_2}$	
t, τ	time, and its dummy variable
u	control vector
V	airspeed; subspace of the original state space
V^M	largest invariant subspace contained in $e^{\perp}$
$V^{\perp}$	orthogonal complement of V
$\vec{V}$	inertial velocity
$V_{\bar{c}/4}$	velocity of the airfoil one-quarter chord point
v_i	basis for subspace V, $i = 1,\ldots,k$
$\hat{v}_i$	basis for subspace $V^{\perp}$, $i = k+1,\ldots,n$
W_{cycle}	net work done on airfoil system per cycle
x	state vector
x_A	column vector of aerodynamic state variables

x_1	nondimensionalized distance of main section center of gravity from e.a.
x_α	nondimensionalized distance of center of gravity from e.a.
Y	column vector of plunge, pitch, and flap displacements
z	redefined state vector
α	angle of attack, positive nose up
α_1, α_2	coefficients in two-term exponential approximation to the Wagner functon
β	flap deflection angle, positive tail down
β_c	commanded control surface deflection
β_1, β_2	coefficients in exponent in two-term exponential approximation to the Wagner function
Φ_i	functions defined in Appendix C, $i = 1,\ldots,12$
ϕ_j	phase angle of aerodynamic forces and motion variables
Φ (Vt/b)	Wagner function
$\boldsymbol{\varphi}$	value of Θ at the flap hinge line
Θ	symbol defined in Figure 1
ρ	air density
ω	circular frequency

ω_n	natural frequency
ω_r	reference frequency
$\subset$	is contained in
$\notin$	is not an element of

Superscripts

$(\ )'$	$d(\ )/d\tau$
$(\ )''$	$d^2(\ )d\tau^2$
$(\dot{\ })$	$d(\ )/dt$
$(\ddot{\ })$	$d^2(\ )/dt^2$
$(\ )_e$	equilibrium value

INTRODUCTION

The design of modern high-performance aircraft is toward increased aerodynamic efficiency, decreased structural weight, and higher flight speeds. Preliminary designs often exhibit a flutter instability within the desired operating envelope of the aircraft. Passive methods which have been used to solve the flutter problem include added structural stiffness, mass balancing, and speed restrictions. These methods may result in significant weight penalties. Studies by Boeing (ref. 1) show that weight penalties as high as 2 to 4% of the total structural weight may be required to solve the flutter problem passively by increasing the structural stiffness. Therefore, there is considerable interest in alternative methods of increasing the flutter speed beyond the original unaided value.

Within the past few years the advances in active control technology have made the application of active flutter suppression systems feasible, resulting in significantly smaller performance penalties. Control systems used to alter the aeroelastic response have been implemented successfully on several aircraft. Applications have been augmentation of static stability, ride quality improvement, maneuver load reduction, and suppression of structural loads induced by atmospheric turbulence. Harris and Rickard (ref. 2) list the present application experience of active control technology on experimental, commercial, and military aircraft. Active flutter suppression is fundamentally different from the preceding applications since the structural stability of the flexible vehicle is at stake. Loss of the former four items would result in

deteriorated performance or shortened vehicle life, while loss of an active flutter suppression system when flying above the flutter speed would result in loss of the aircraft. Harris and Rickard (ref. 2) list the severity of the situation associated with degradation of various active control functions. To date there have been many analytical studies and successful wind tunnel demonstrations of active flutter control systems. See references 3 through 7. An active flutter suppression system installed on a full-scale B-52 test airplane has been successfully flight tested (ref. 8). This was the first time an aircraft had been flown above its flutter speed relying entirely on an active flutter control system to supplement the structural damping. The flight was an important step in the acceptance and implementation of this new technology into future aircraft designs.

Active flutter suppression is a method of flutter prevention employing a control surface the deflection of which is commanded by a suitable control law. The control law is the relationship between the motion of the main airfoil surface and the control surface deflection. The control law is determined by applying methods commonly used in control system theory. The two most common methods of control law synthesis are the application of optimal control theory (ref. 9) and the aerodynamic energy method (ref. 10). It is desired here to make use of the latter method.

Flutter is an aeroelastic self-excited unstable vibration in which the airstream energy is absorbed by the lifting surface. The motion involves both bending and torsional components which are basically simple harmonic oscillations with a unique flutter frequency. Classical

flutter will not occur if either the bending or torsion components of the motion are suppressed. Figure 4 illustrates the qualitative nature of the phase relationships during a cycle of motion at the flutter condition. Displacement versus time is plotted for a streamwise airfoil section. At the flutter condition plunge is at or near a maximum where pitch is at or near a minimum. Since the lift acts in the same direction as the plunging velocity and is in phase with the pitching motion the work done by the airstream on the structure is positive, i.e., energy is transferred into the structure. Flutter is the point at which the net positive work is exactly balanced by the damping forces in the system. The motion will diverge when the total work per cycle done by all forces in the system is positive.

The aerodynamic energy method (ref. 10) of active flutter suppression is based on the fact that the flutter instability is inherently connected to the nature of the aerodynamic forces acting on the airfoil. At flutter these forces allow a transfer of energy from the surrounding airstream into the airfoil. Flutter can be suppressed at any flight configuration provided the control surfaces can be deflected in a manner which alters the overall nature of the aerodynamic forces. In particular, the magnitude and phase relationships of the lift and pitching moment with the plunging rate and pitch rate respectively are modified such that energy is transferred from the airfoil to the surrounding airstream.

I. AIRFOIL EQUATIONS OF MOTION

The two-dimensional airfoil which will be analyzed is shown in figure 2. It has a trailing edge control surface which is aerodynamically unbalanced (hinge line at leading edge of control surface). The linear and torsional springs, K_h and K_α, are mounted at the shear center of the airfoil cross-section and provide restraining forces in the plunging (h), and pitching (α) degrees of freedom. The torsional spring K_β restrains the trailing edge control surface deflection. The origin of the coordinate system coincides with the shear center when the airfoil is in its undeflected position. The plunging displacement h, is measured positive down. The total lift on the airfoil L, is defined positive up while the pitching moment of the entire airfoil about the one quarter chord point M, is positive in the nose-heavy sense. The equations of motion are derived in Appendix A as

$$M\ddot{Y} + K\,Y = \begin{bmatrix} -L \\ -M_{e.a.} \\ -T-T_s \end{bmatrix} \tag{1.1}$$

where

$$Y = \begin{bmatrix} \frac{h}{b} \\ \alpha \\ \beta \end{bmatrix}$$

The M and K matrices are

$$M = \begin{bmatrix} bm & S_\alpha & S_\beta \\ bS_\alpha & I_\alpha & I_\beta+S_\beta bc \\ bS_\beta & I_\beta+S_\beta bc & I_\beta \end{bmatrix}$$

$$K = \begin{bmatrix} bK_h & 0 & 0 \\ 0 & K_\alpha & 0 \\ 0 & 0 & K_\beta \end{bmatrix}$$

Equation (1.1) describes a three degree of freedom model.

The system description is complete for the open loop (uncontrolled) system when the aerodynamic loads L, M, and T have been specified. These aerodynamic loads are derived in Appendix B. The closed loop (controlled) system will require an additional flap hinge torque T_s to drive the flap to its commanded position.

II. THE UNSTEADY AERODYNAMIC LOADS

Linearized, unsteady aerodynamic theory provides the basis for the computation of the unsteady aerodynamic loads acting on the airfoil. Kussner & Schwarz (ref. 11) apply this theory deriving formulas which give the pressure distribution of the wing and the aerodynamic reactions of oscillating elevators and tabs for any position of the elevator hinge with respect to the elevator leading edge. The wing analyzed in reference 11 has a total of six degrees of freedom whereas the present analysis involves the three degrees of freedom shown in Fig. 1. The linearization of the problem as presented in reference 11 allows the total aerodynamic loads to be found by superposition of the forces and moments associated with each degree of freedom. Consequently the analysis of Kussner & Schwarz (ref. 11) can easily be restricted to the present three degree of freedom case. Kussner & Schwarz (ref. 11) employ two-dimensional thin airfoil theory which is based on incompressible flow over an airfoil of zero thickness. Also the pitching, plunging, and control surface oscillations are harmonic with small amplitudes. In the present study the wing has an elevator pivoted at the elevator leading edge (aerodynamically unbalanced) and is replaced by a plate with a single bend at the hinge line. Under the usual assumption of thin airfoil theory the actual airfoil profile is replaced by its mean chord which in the rest position lies on the x-axis extending from $x = -1$ (leading edge) to $x = 1$ (trailing edge) as shown in figure 1.

The total lift, total pitching moment about the one quarter chord point, and the elevator hinge moment are derived from reference 11 in Appendix B as

$$L = \pi\rho b^2 \left\{ [b]\frac{\ddot{h}}{b} + \left[\frac{b}{2}\right]\ddot{\alpha} + \left[\frac{b}{2\pi}\ \Phi_4\right]\ddot{\beta} + [2V]\frac{\dot{h}}{b} + [3V]\dot{\alpha} \right.$$

$$\left. + \left[\frac{V(\Phi_3+\Phi_2)}{\pi}\right]\dot{\beta} + \left[\frac{2V^2}{b}\right]\alpha + \left[\frac{2V^2\Phi_1}{\pi b}\right]\beta - \left[\frac{2V\alpha_1}{b}\right]B_1 - \left[\frac{2V\alpha_2}{b}\right]B_2 \right\} \quad (2.1)$$

$$M = \pi\rho b^2 \left\{ \left[\frac{b^2}{2}\right]\frac{\ddot{h}}{b} + \left[\frac{3b^2}{8}\right]\ddot{\alpha} + \left[\frac{b^2}{4\pi}\ \Phi_7\right]\ddot{\beta} + [Vb]\dot{\alpha} \right.$$

$$\left. + \left[\frac{Vb}{2\pi}\ \Phi_6\right]\dot{\beta} + \left[\frac{V^2}{\pi}\ \Phi_5\right]\beta \right\} \quad (2.2)$$

$$T = \pi\rho b^2 \left\{ \left[\frac{b^2}{2\pi}\ \Phi_4\right]\frac{\ddot{h}}{b} + \left[\frac{b^2}{4\pi}\ \Phi_7\right]\ddot{\alpha} + \left[\frac{b^2}{4\pi^2}\ \Phi_{12}\right]\ddot{\beta} \right.$$

$$+ \left[\frac{Vb}{\pi}\ \Phi_8\right]\frac{\dot{h}}{b} + \left[\frac{Vb}{\pi}\left(\frac{\Phi_9}{2} + \Phi_8\right)\right]\dot{\alpha} + \left[\frac{Vb}{2\pi^2}\ (\Phi_{11}+\Phi_2\Phi_8)\right]\dot{\beta} \quad (2.3)$$

$$\left. + \left[\frac{V^2}{\pi}\ \Phi_8\right]\alpha + \left[\frac{V^2}{\pi^2}\ (\Phi_{10} + \Phi_1\Phi_8)\right]\beta - \left[\frac{V\alpha_1}{b}\right]A_1 - \left[\frac{V\alpha_2}{b}\right]A_2 \right\}$$

where Φ_1 through Φ_{12} are listed in Appendix C.

III. THE STATE SPACE EQUATIONS OF MOTION

The state space representation of the equations of motion (eq. 1.1) with no control input is a set of ten first-order simultaneous differential equations of the form

$$\dot{x}(t) = f[x(t), t] \tag{3.1}$$

where x(t) is a real ten-dimensional column vector which is the state of the system and t is the time variable. Equation 1.1 is transformed into the following state space representation

$$\dot{x} = \begin{bmatrix} \ddot{Y} \\ \dot{Y} \\ \dot{x}_A \end{bmatrix} = \begin{bmatrix} A_{11} & A_{12} & A_{13} \\ A_{21} & A_{22} & A_{23} \\ A_{31} & A_{32} & A_{33} \end{bmatrix} \begin{bmatrix} \dot{Y} \\ Y \\ x_A \end{bmatrix} = Ax \tag{3.2}$$

where $Y = [h/b \quad \alpha \quad \beta]^T$ and $x_A = [B_1 \quad B_2 \quad A_1 \quad A_2]^T$ are the four aerodynamic state variables defined by equations B.21 through B.24. The A_{11} through A_{33} sub-matrices are derived in appendix D.

The stability of the airfoil system can be determined by examining the eigenvalues of the A matrix. The system is stable if the real part of each eigenvalue is negative. The flutter instability occurs when the real part of any eigenvalue becomes positive.

A Fortran IV program was written to assemble the 10x10 A matrix in equation 3.2 and solve for the eigenvalues and eigenvectors using the IMSL subroutine EIGRF. The correctness of the state model was verified using the three degree-of-freedom parameters listed in table III-3 of

reference 12. The corresponding parameters used to construct the M and K matrices are shown in table 1. The resulting locus of roots shown in figure 3 closely match the locus of roots given by figure III-1 in reference 12. The open loop flutter speed of 893 ft/sec. is near the 900 ft/sec. open loop flutter speed given by reference 12.

The pitching, plunging, and flap modes are identified as the eigenvectors whose largest component corresponds to the pitch, plunge, and flap motions, respectively. The pitch, plunge, and flap components are non-dimensional with plunge scaled as h/b. Thus, the three quantities are comparable enabling the largest component to be easily identified. The aerodynamic modes are identified in the same manner as the pitching, plunging, and flap modes. The system modes then are not "pure" modes. For instance, the pitching mode consists primarily of torsional motion with lesser amounts of bending and flap motions.

IV. THE ENERGY ANALYSIS

The stability of the system is determined by the net work done per cycle by the forces acting on the system. If the sign of the net work is positive, energy is being transferred from the surroundings to the system resulting in an unstable condition. The system is dissipating energy (i.e., stable) when the net work is negative.

Using the work-energy concept from elementary mechanics it is easy to relate the forces acting on the system to the resulting changes in kinetic energy. This is stated as

$$\dot{E} = m\left(\frac{d\vec{V}}{dt}\right)\cdot\vec{V} = \vec{F}\cdot\vec{V} \tag{4.1}$$

where $\dot{E}$ represents the time rate of change of kinetic energy for a particle; m, the particle mass; $\vec{F}$, the resultant force; and $\vec{V}$ the inertial velocity. Application of equation 4.1 to the three degree of freedom airfoil is now considered. Represent the airfoil as a collection of points. The velocity of any point on the airfoil (see Figure 6) is

$$\vec{V}(x) = -\left\{\dot{h} - [b(d-1/2)-x]\dot{\alpha}\right\}\vec{j},\ -\frac{b}{2} \leq x \leq b(d+c-1/2) \tag{4.2}$$

$$\vec{V}(x) = -\left\{\dot{h} - [b(d-1/2)-x]\dot{\alpha} + [x-b(d+c-1/2)]\dot{\beta}\right\}\vec{j},$$
$$b(d+c-1/2) \leq x \leq \frac{3b}{2} \tag{4.3}$$

Consider a small element of the airfoil, dx. Let P_u represent the pressure on the upper surface of the element and P_l the pressure on the lower surface of the element (see Figure 6). $(P_l - P_u)$ represents the

lift of the element, positive up. The rate at which kinetic energy is being transferred from the surrounding airstream to the airfoil, due to the action of the aerodynamic forces is represented as

$$\dot{E}_{aero} = -\int_{-b/2}^{b(d+c-1/2)} (P_l - P_u)\left\{\dot{h} - [b(d-1/2) - x]\dot{\alpha}\right\} dx$$

$$-\int_{b(d+c-1/2)}^{3b/2} (P_l - P_u)\left\{\dot{h} - [b(d-1/2) - x]\dot{\alpha} + [x - b(d+c-1/2)]\dot{\beta}\right\} dx$$

or (4.4)

$$\dot{E}_{aero} = -L[\dot{h} - b(d-1/2)\dot{\alpha}] - M\dot{\alpha} - T\dot{\beta}$$

where the quantity $[\dot{h} - b(d-1/2)\dot{\alpha}]$ is the velocity of the one-quarter chord point, positive down.

The forces exerted by the bending, torsional, and flap hinge restraining springs also contribute to the rate of kinetic energy transfer into the system. This contribution is given by

$$\dot{E}_{spring} = -K_h h\dot{h} - K_\alpha \alpha\dot{\alpha} - K_\beta \beta\dot{\beta} \tag{4.5}$$

Addition of the equations 4.4 and 4.5 gives the total instantaneous kinetic energy rate for the open loop (uncontrolled) system as

$$\dot{E}_{total} = \dot{E}_{aero} + \dot{E}_{spring} \tag{4.6}$$

If $\dot{E}_{total}$ is negative the system is losing kinetic energy with time (i.e., the motion is decaying) at a particular instant of time. A positive value of $\dot{E}_{total}$ indicates the system is gaining kinetic energy

(i.e., the motion is increasing) at that particular time.

The net work done on the system per cycle is found by integrating equation 4.6 over one cycle of motion as

$$W_{cycle} = \int_0^{\frac{2\pi}{\omega}} \dot{E}_{aero}\, dt + \int_0^{\frac{2\pi}{\omega}} \dot{E}_{spring}\, dt \tag{4.7}$$

The second term in equation 4.7 is equal to zero since the spring forces are conservative. Rewrite equation 4.7 as

$$W_{cycle} = \int_0^{\frac{2\pi}{\omega}} \dot{E}_{aero}\, dt \tag{4.8}$$

As the first step in evaluating equation 4.6 and 4.8 represent the aerodynamic loads and motion variables as

$$j = A_j \cos(\omega t + \phi_j) \;;\; j = L,\ M,\ T,\ h, \alpha, \beta, \dot{h}, \dot{\alpha}, \dot{\beta} \tag{4.9}$$

For the non-oscillatory modes equation 4.9 is rewritten as

$$j = A_j \cos\phi_j \quad \begin{cases} j = L, M, T, h, \alpha, \beta, \dot{h}, \dot{\alpha}, \dot{\beta} \\ \phi_j = 0, \pi \end{cases} \tag{4.10}$$

Substitution of equation 4.10 into equation 4.6 yields the kinetic energy rate expression for the non-oscillatory modes of the open loop system as

$$\dot{E}_{no}=-A_L\dot{A}_h\cos\phi_L\cos\dot{\phi}_h+A_L\dot{A}_\alpha b(d-1/2)\cos\phi_L\cos\dot{\phi}_\alpha-A_M\dot{A}_\alpha\cos\phi_M\cos\dot{\phi}_\alpha$$
$$-A_T\dot{A}_\beta\cos\phi_T\cos\dot{\phi}_\beta-K_hA_hA_h\dot{A}_h\cos\phi_h\cos\dot{\phi}_h-K_\alpha A_\alpha\dot{A}_\alpha\cos\phi_\alpha\cos\dot{\phi}_\alpha-K_\beta A_\beta\dot{A}_\beta\cos\phi_\beta$$
$$\cos\phi_\beta \tag{4.11}$$

Combination of equations 4.10, 4.4 and 4.8 yields the net work done per cycle for the oscillatory modes of the open loop system as

$$W_{cycle} = \frac{\pi}{\omega}\,[-A_L\dot{A}_h(\cos\phi_L\cos\dot{\phi}_h+\sin\phi_L\sin\dot{\phi}_h)+A_L\dot{A}_\alpha b(d-1/2)$$
$$(\cos\phi_L\cos\dot{\phi}_\alpha+\sin\phi_L\sin\dot{\phi}_\alpha)-A_M\dot{A}_\alpha(\cos\phi_M\cos\dot{\phi}_\alpha+\sin\phi_M\sin\dot{\phi}_\alpha)-A_T$$
$$\dot{A}_\beta(\cos\dot{\phi}_\beta\cos\phi_T+\sin\dot{\phi}_\beta\sin\phi_T)] \tag{4.12}$$

With the introduction of control to the system there is an additional servo hinge torque T_s that contributes to the rate of kinetic energy transfer into the system. The contribution due to T_s is

$$\dot{E}_{control} = -\,T_s\dot{\beta} \tag{4.13}$$

In the closed loop system the servo provides control of the flap angle, thus the flap spring is not needed and equation 4.5 becomes

$$\dot{E}_{spring} = -K_h h\dot{h} - K_\alpha \alpha\dot{\alpha} \tag{4.14}$$

Addition of equations 4.4, 4.13 and 4.14 gives the total instantaneous kinetic energy rate for the closed loop (controlled) system as

$$\dot{E}_{total} = \dot{E}_{aero} + \dot{E}_{spring} + \dot{E}_{control} \tag{4.15}$$

Represent T_s in the form given by equation 4.9 as

$$T_s = A_{T_s} \cos(\omega t + \phi_{T_s}) \tag{4.16}$$

Thus, equations 4.11 and 4.12 are modified for the closed loop system by the changes introduced in equations 4.13 and 4.14. The kinetic energy rate expression for the non-oscillatory modes of the closed loop system is then given by

$$\begin{aligned}\dot{E}_{no} = &-A_L A_{\dot{h}} \cos\phi_L \cos\phi_{\dot{h}} + A_L A_{\dot{\alpha}}\, b\,(d - 1/2) \cos\phi_L \cos\phi_{\dot{\alpha}} \\ &-A_M A_{\dot{\alpha}} \cos\phi_M \cos\phi_{\dot{\alpha}} - (A_T + A_{T_s}) A_{\dot{\beta}} \cos\phi_T \cos\phi_{\dot{\beta}} \\ &-K_h A_h A_{\dot{h}} \cos\phi_h \cos\phi_{\dot{h}} - K_\alpha A_\alpha A_{\dot{\alpha}} \cos\phi_\alpha \cos\phi_{\dot{\alpha}}\end{aligned} \tag{4.17}$$

and the net work done per cycle for the oscillatory modes of the closed loop system is

$$W_{cycle} = \frac{\pi}{\omega} [-A_L A_{\dot{h}} (\cos \phi_L \cos \phi_{\dot{h}} + \sin \phi_L \sin \phi_{\dot{h}}) + A_L A_{\dot{\alpha}} b (d - 1/2) (\cos \phi_L \cos \phi_{\dot{\alpha}} + \sin \phi_L \sin \phi_{\dot{\alpha}}) - A_M A_{\dot{\alpha}} (\cos \phi_M \cos \phi_{\dot{\alpha}} + \sin \phi_M \sin \phi_{\dot{\alpha}}) - (A_T + A_{T_s}) A_{\dot{\beta}} (\cos \phi_{\dot{\beta}} \cos \phi_T + \sin \phi_{\dot{\beta}} \sin \phi_T)] \tag{4.18}$$

The requirement for stability of the open loop or closed loop system is

$$\dot{E}_{no} < 0$$

and (4.19)

$$W_{cycle} < 0$$

Equations 4.11 and 4.12 were implemented in the computer program described in section III. $\dot{E}_{no}$ and W_{cycle} were computed for the same system analyzed in section III. The results were shown in figures 7 and 8. Figure 7 shows $-W_{cycle}$ /Period versus velocity for the pitching, plunging, and flap modes. Figure 8 shows $-\dot{E}_{no}$ versus velocity for the four modes corresponding to the aerodynamic state variables.

V. METHODS OF CLOSED LOOP CONTROL

The concept of closed loop control of flutter is straightforward in theory (see Figure 9). The first step of the control scheme involves the measurement of the motion components (state variables) needed to construct the control law. The flap command is formed by the control law and fed into the servo. The servo then deflects the flap at the proper rate and phase, thus providing aerodynamic forces and moments that oppose the motion of the wing.

The flutter suppression system used in the present study does not include servo dynamics, i.e., β and β_c are identical. For this type of system the flap would respond instantaneously to the command flap position with the same magnitude as the command. There are some subtle analytical difficulties that can be encountered in the implementation of this type of system. These potential difficulties will be discussed later.

Of course, any actual flutter suppression system would require a servo to deflect the control surface. The servo transfer function will invariably introduce phase lags and amplitude changes between the desired and actual control deflections. Although these phase lags and amplitude changes may be small they can easily deprive the system of its effectiveness. Another drawback associated with the introduction of a servo in the feedback loop is the additional states required to model the servo. Consider the servo block diagram representation shown in figure 10. The compensation block includes integral, proportional, and rate control terms which operate on the error ε. Integral control

is needed to eliminate steady state errors and rate control provides lead in the control deflection. The transfer function between the torque applied to the control surface and the actual control surface deflection is represented by a typical second-order block. The introduction of integral control requires the addition of three new states to the original state vector as

$$x_{new} = [x_{old} \,\vdots\, \int(h/b) \,\vdots\, \int\alpha \,\vdots\, \int\beta \quad] \tag{5.1}$$

Implementation of the perfect model following system (i.e., $\beta = \beta_c$) is not as straightforward as it may seem at first glance. Consider the simple two-degree of freedom mass-spring system shown in figure 11. The behavior of the three-degree of freedom airfoil system is more easily understood in terms of the simpler two degree of freedom mass-spring system. the mass-spring notation m_1, m_2, k_2, and x_2 is analogous to the airfoil notation m_1, m_2, k_β, and β respectively.

Application of Newton's second law to each body separately yields the equations of motion (free vibration case) for the mass- spring system as

$$\begin{bmatrix} m_1 & 0 \\ m_2 & m_2 \end{bmatrix} \begin{bmatrix} \ddot{x}_1 \\ \ddot{x}_2 \end{bmatrix} + \begin{bmatrix} k_1 & -k_2 \\ 0 & k_2 \end{bmatrix} \begin{bmatrix} x_1 \\ x_2 \end{bmatrix} = \begin{bmatrix} 0 \\ 0 \end{bmatrix} \tag{5.2}$$

If the spring stiffness k_2 approaches infinity (i.e., m_1 and m_2 are connected by a massless rigid rod; $x_2 = 0$) the

natural frequency of the system is

$$\omega_n = \sqrt{\frac{k_1}{m_1 + m_2}} \tag{5.3}$$

Reduction of the two degree of freedom system to a one degree of freedom system by deleting the second rows and columns in equation 5.2 yields the natural frequency as

$$\omega_n = \sqrt{\frac{k_1}{m_1}} \tag{5.4}$$

The prediction for ω_n using equation 5.3 and equation 5.4 are different. This occurs because the mass and stiffness matrices in equation 5.2 are not symmetrical.

The constraining force F_s is analogous to the servo torque T_s applied to the flap in the three degree of freedom airfoil problem. It is of interest to examine the behavior of the system for the two cases where F_s is applied internally as shown in Figure 11 or F_s is applied externally on body 2. The equations of motion for the system with F_s applied <u>internally</u> are

$$\begin{bmatrix} m_1 & 0 \\ m_2 & m_2 \end{bmatrix} \begin{bmatrix} \ddot{x}_1 \\ \ddot{x}_2 \end{bmatrix} + \begin{bmatrix} k_1 & -k_2 \\ 0 & k_2 \end{bmatrix} \begin{bmatrix} x_1 \\ x_2 \end{bmatrix} = \begin{bmatrix} -1 \\ 1 \end{bmatrix} F_s \tag{5.5}$$

By imposing the restriction of no relative displacement between body 1 and body 2 ($x_2 = 0$), equation 5.5 reduces to

$$m_1\ddot{x}_1 + k_1 x_1 = - F_s \tag{5.6a}$$

$$m_2\ddot{x}_1 = F_s \tag{5.6b}$$

Substituting equation 5.6b into equation 5.6a yields

$$(m_1+m_2)\ddot{x}_1 + k_1x_1 = 0 \tag{5.7}$$

Thus with F_s applied internally the natural frequency of the system is given by equation 5.3 as expected. With F_s applied <u>externally</u> to body 2 the equations of motion for the system are

$$\begin{bmatrix} m_1 & 0 \\ m_2 & m_2 \end{bmatrix} \begin{bmatrix} \ddot{x}_1 \\ \ddot{x}_2 \end{bmatrix} + \begin{bmatrix} k_1 & -k_2 \\ 0 & k_2 \end{bmatrix} \begin{bmatrix} x_1 \\ x_2 \end{bmatrix} = \begin{bmatrix} 0 \\ 1 \end{bmatrix} F_s \tag{5.8}$$

Applying the constraint $x_2 = 0$ equation 5.8 reduces to

$$m_1\ddot{x}_1 + k_1x_1 = 0 \tag{5.9a}$$

$$m_2\ddot{x}_1 = F_s \tag{5.9b}$$

From equation 5.9a the predicted natural frequency is the same as given by equation 5.4.

It is clear then, that internal and external application of the constraint force are not equivalent in terms of the system dynamic behavior. In terms of the three degree of freedom airfoil problem the preceeding analysis demonstrates that introduction of the control law, $\beta = \beta_c$, into the open loop system requires the addition of an internal hinge torque. This torque would assume the value necessary to force the flap deflection equal to the commanded flap position.

Application of a general control law to the simple mass- spring system is now considered. The kinematic control law is constructed as

a linear combination of the states x_1 and x_2 as

$$x_2 = nx_1 + \ell\dot{x}_1 \tag{5.10}$$

The kinematic control law represented by equation 5.10 could be implemented by rederiving the equations of motion. A more expeditious method employed here involves the use of geometric theory discussed in reference 13.

With the introduction of control the dynamical system is described by

$$\dot{x} = Ax + bu \tag{5.11}$$

where x and A are defined in section three, u is the control vector, and b is a constant column matrix. The control vector u is a linear function of the state vector x and is represented as

$$u = fx \tag{5.12}$$

Substituting equation 5.12 into equation 5.11 yields the augmented system representation as

$$\dot{x} = (A+bf)x \tag{5.13}$$

Given A, b, and the kinematic control law, geometric theory can be implemented to determine a feedback maxtrix f. Geometric theory provides a method of computing the feedback matrix f such that a given subspace V is invariant under (A+bf). That is, the feedback matrix f insures that the system motion remains within the subspace V provided $f \cdot x$ is the only control used. The subspace V is defined by the kine-

matic control law.

The method of determining f using geometric theory is now illustrated for the simple mass- spring system (figure 11) with the control law given by equation 5.10. Let the mass of both body 1 and body 2 be denoted by m. The equations of motion for the system (equation 5.5) become

$$\begin{bmatrix} m & 0 \\ m & m \end{bmatrix} \begin{bmatrix} \ddot{x}_1 \\ \ddot{x}_2 \end{bmatrix} + \begin{bmatrix} k_1 & -k_2 \\ 0 & k_2 \end{bmatrix} \begin{bmatrix} x_1 \\ x_2 \end{bmatrix} = \begin{bmatrix} -1 \\ 1 \end{bmatrix} F_s \tag{5.14}$$

Define the state variables as

$$z = \begin{bmatrix} z_1 = x_1 \\ z_2 = \dot{x}_2 \\ z_3 = \dot{x}_1 \\ z_4 = x_2 \end{bmatrix} \tag{5.15}$$

Rewrite equation 5.14 as

$$\begin{bmatrix} \ddot{x}_1 \\ \ddot{x}_2 \end{bmatrix} = \begin{bmatrix} \frac{-k_1}{m} & \frac{k_2}{m} \\ \frac{k_1}{m} & \frac{-2k_2}{m} \end{bmatrix} \begin{bmatrix} x_1 \\ x_2 \end{bmatrix} + \begin{bmatrix} \frac{-1}{m} \\ \frac{2}{m} \end{bmatrix} F_s \tag{5.16}$$

Define P and u as

$$P = \frac{k_1}{m} = \frac{k_2}{m} = \frac{k}{m}$$

and

$$u = \frac{F_s}{m} \tag{5.17}$$

Rewriting equation 5.16 in the standard state form yields

$$\dot{z} = Az + bu \tag{5.18}$$

where

$$A = \begin{bmatrix} 0 & 0 & 1 & 0 \\ 0 & 0 & 0 & 1 \\ -P & P & 0 & 0 \\ P & -2P & 0 & 0 \end{bmatrix}$$

and

$$b = \begin{bmatrix} 0 \\ 0 \\ -1 \\ 2 \end{bmatrix}$$

Now introduce the constraint (equation 5.10 with a = 1) as

$$z_2 = z_1 + \ell z_3 \tag{5.19}$$

The geometric statement is

$$z_2 - z_1 - \ell z_3 = 0 \tag{5.20}$$

or

$$z \cdot e = 0 \tag{5.21}$$

where

$$e = [-1 \;\; 1 \;\; -\ell \;\; 0]^T \tag{5.22}$$

By inspection the subspace orthogonal to e, denoted by $e^{\perp}$ is

$$\left\{ \begin{bmatrix} 0 \\ 0 \\ 0 \\ 1 \end{bmatrix}, \begin{bmatrix} 1 \\ 1 \\ 0 \\ 0 \end{bmatrix}, \begin{bmatrix} 0 \\ \ell \\ 1 \\ 0 \end{bmatrix} \right\} = \left\{ e_1, \; e_2, \; e_3 \right\} = e^{\perp} \tag{5.23}$$

We seek a dynamic feedback law $F_s = f \cdot z$ so that the system will move in $e^{\perp}$. In geometric language we want to arrange a control law so that under feedback the subspace $e^{\perp}$ will be an <u>invariant</u> subspace. In this case we say that $e^{\perp}$ is an (A,b) invariant subspace. In some cases it may happen that $e^{\perp}$ is not an (A,b) invariant subspace but that it properly contains such a subspace. To account for this possibility we make use of an algorithm from [13, see Theorem 1] and generate the largest (A,b) invariant subspace (say V^M) contained in $e^{\perp}$.

For this problem it happens that $V^M = e^{\perp}$; that is the whole null space of e ($e^{\perp}$) is an invariant subspace of (A,b). For V to be invariant under (A+bf) we require that

$$[(A+bf)e_i \cdot e] = 0 \quad , \; i=1,2,3 \tag{5.24}$$

or

$$bfe_i \cdot e = -Ae_i \cdot e \quad , \; i=1,2,3 \tag{5.25}$$

Application of equation 5.25 yields the three equations for the elements of the feedback matrix f as

$$i=1: \qquad f_4 = -\ 1/\ell \tag{5.26}$$

$$i=2: \qquad f_1+f_2 = 0 \tag{5.27}$$

$$i=3: \qquad \ell(f_3+\ell f_2) = 1 + \ell^2 P \tag{5.28}$$

In general the feedback matrix f is not unique, i.e. there is a whole class of f matrices which make V invariant under (A+bf). The solution of equations 5.26 through 5.28 is not unique. Choose $f_1 = a$, then the feedback matrix solution is

$$f=[f_1\ f_2\ f_3\ f_4]=[a \,\vdots\, -a \,\vdots\, \frac{1}{\ell}+\ell P + \ell a \,\vdots\, \frac{-1}{\ell}] \tag{5.29}$$

Finally the (A+bf) matrix is

$$A+bf=\left[\begin{array}{c|c|c|c} 0 & 0 & 1 & 0 \\ \hline 0 & 0 & 0 & 0 \\ \hline -(P+a) & (P+a) & -\ell(\frac{1}{\ell^2} + P + a) & \frac{1}{\ell} \\ \hline P + 2a & -2\ (P+a) & 2\ell(\frac{1}{\ell^2} + P + a) & \frac{-2}{\ell} \end{array}\right] \tag{5.30}$$

Since the augmented matrix given by (5.30) contains an arbitrary parameter (a), it may seem that the response of the system will depend

on the value of a. The point of the next paragraph is to demonstrate that the part of the dynamics associated with the motion in $e^{\perp}$ is, in fact, independent of the value of a.

From reference 13 it is known that if V is an (A,b) invariant subspace then the image of V under A must be contained in the sum $\{b\} + V$.

$$AV \subset \{b\} + V$$

If $b \in V$ then $AV \subset V$ so that V is invariant with zero feedback. Thus, we suppose that $b \notin V$. Let f_1, and f_2 be two possible feedback matrices. From the generalization of (5.25) we know that if $\{v_1, \cdots v_k\}$ is a basis for V and $\{\hat{v}_{k+1}, \ldots \hat{v}_n\}$ is a basis for $V^{\perp}$ then

$$bfv_i \cdot \hat{v}_j = -Av_i \cdot \hat{v}_j \tag{5.31}$$

If we write the system (5.31) for f_1 and for f_2 then subtract we find

$$b(f_1 - f_2)v_i \cdot \hat{v}_j = 0 \tag{5.32}$$

which can be written as

$$(b \cdot \hat{v}_j) \cdot (d \cdot v_i) = 0 \tag{5.33}$$

where $d = f_1 - f_2$. Since $b \notin V$ then for some j $(b \cdot \hat{v}_j) \neq 0$. Thus, we must have $d \cdot v_i = 0$, $i = 1, \ldots, k$. Geometrically, this means that the vector d is an element of $V^{\perp}$, the orthogonal complement of V. Finally, let P be the matrix that projects vectors along $V^{\perp}$ onto V. Then the dynamics of the system in V are represented by the matrix

$(A+bf)P$. Now compute

$$(A+bf_2)P = (A+bf_1+bd)P \tag{5.34}$$

$$= (A+bf_1)P+bdP$$

However, since $Px \in V$ and $d \in V^{\perp}$ the last term is identically zero. Thus

$$(A+bf_2)P = (A+bf_1)P \tag{5.35}$$

and we have proved that any two feedback matrices that make V invariant produce the same dynamic response <u>in</u> <u>V</u>. Responses in $V^{\perp}$ do differ but they are not of concern here.

A method of introducing the control law into the open loop system (i.e., closing the loop) using geometric theory has been demonstrated for a simple mass- spring system. This method will be applied to the airfoil problem in the next section.

VI. CLOSED LOOP ANALYSIS

The geometric technique introduced in the previous section is applied to a two DOF airfoil in this section. The control law derived by Nissim (ref. 10) for trailing- edge control only will be implemented.

Nissim's design procedure doesn't include the flap degree of freedom. That is, Nissim's rigid two- dimensional strip has two degrees of freedom, translation (bending) and rotation (torsion). Thus, to apply Nissim's control law the airfoil analyzed in section three is reduced to a two DOF airfoil by discarding the flap mode. This is accomplished by setting the flap inertia to zero. The value of the total mass of the airfoil is not changed. This redistribution of mass alters the pitching and plunging frequencies at zero velocity as shown below.

	3 DOF	2 DOF (zero flap inertia)
Pitching:	109.23 rad/sec.	111.23 rad/sec.
Plunging:	48.1 rad/sec.	48.32 rad/sec.

The locus of roots for the two DOF (zero flap inertia) airfoil and the corresponding work per cycle versus velocity plot is shown in figures 12 and 13 respectively. The pitching mode becomes unstable between 890 ft./sec. and 900 ft./sec.

The control law given by Nissim in reference 6 is

$$\beta_c = [-0.35 \ -1.9] \begin{bmatrix} \frac{h}{b} \\ \alpha \end{bmatrix} + \frac{1}{\omega_r} [0.35 \ 0.1] \begin{bmatrix} \frac{\dot{h}}{b} \\ \dot{\alpha} \end{bmatrix} \tag{6.1}$$

where ω_r is a reference frequency near the open loop flutter frequency. A value of 72.3 rad/sec was chosen. The matrix elements -0.35, -1.9, 0.35, and 0.1 are fixed for 20 percent chord trailing edge flap control and wing displacement measured at 30 percent chord. The same geometry was used here.

The procedure for implementation of equation 6.1 using the geometric technique is the same as outlined for the simple mass- spring example in the previous section. The vector space operations required to find a feedback matrix f were performed using the appropriate portions of the Fortran IV program used in reference 13. The required inputs to the program are the open loop system matrix A, the control matrix b, and the constraint vector H. The output is a set of linear equations for the elements of the feedback matrix. There are generally more equations than the number of elements in the feedback matrix, thus there is not a unique solution. A linear least squares solution technique using the IMSL subroutine LLSQF was employed to find a solution.

The particular inputs used for this example are

$$H = \left[\frac{-0.35}{\omega_r} \; \frac{-0.1}{\omega_r} \;\; 0 \;\; 0.35 \;\; 1.9 \;\; 1 \;\; 0 \;\; 0 \;\; 0 \;\; 0\right]^T$$

$$A = A_{oL} \tag{6.2}$$

$$b = [-b_1 \;\; 0 \;\; 0 \;\; 0 \;\; 0 \;\; 0 \;\; 0 \;\; 0]^T$$

where A_{oL} is the open loop A matrix and b_1 is the last column of the matrix $[M' + \pi\rho b^2 \; z_1 \;]$. The control u is the scalar T_s given by

$$u = T_s = f \; x \tag{6.3}$$

The root locus and work per cycle versus velocity plots for this example are shown in figures 14 and 15 respectively. Nissim's control law actually destabilizes the system leading to an unstable pitching mode throughout the entire range of velocities shown. Hence, Nissim's control law (eq. 6.1) is seriously deficient in the pitch degree of freedom, causing the torisonal damping to decrease from its open loop value.

VII. CLOSED LOOP CONTROL LAW SYNTHESIS

This section introduces a method of control law synthesis aimed at increased energy dissipation near the flutter speed of the unstable mode. Although a control law designed for a particular mode near flutter may drive other system modes unstable, it may not be possible to design a control law which guarantees energy dissipation for all modes.

Neglecting the contribution due to aerodynamic hinge torque and servo torque, the change in kinetic energy per cycle is

$$E = -\int_0^{2\pi/\omega} (M \cdot \dot{\alpha} + L \cdot V_{\frac{\bar{c}}{4}}) dt \tag{7.1}$$

where $V_{\bar{c}/4}$ represents the velocity of the one-quarter chord point of the airfoil. Approximate the variation of ΔE with a small perturbation of a control law component l_i by the first term in a Taylor series expansion as

$$\Delta E = \Delta E(\hat{l}_i + \Delta l_i) - \Delta E(\hat{l}_i) = \frac{\Delta \partial E}{\partial l_i}\bigg|_{\hat{l}_i} \Delta l_i \quad , \; i = 1,2,3,4 \tag{7.2}$$

where $\hat{l}_i$ is the initial value of the control law component and Δl_i is a small perturbation. The criterion for stability is

$$\frac{\partial \Delta E}{\Delta l_i}\bigg|_{\hat{l}_i} \Delta l_i \quad < \; 0 \quad , \quad i = 1,2,3,4 \tag{7.3}$$

It may be very difficult to obtain an analytical expression for $\partial\Delta E/\partial l_i$. Alternatively it may be approximated numerically as

$$\frac{\partial\Delta E}{\partial l_i} = \frac{\Delta\ E(\hat{l}_i+\Delta l_i)-\Delta E(\hat{l}_i)}{\Delta l_i} \tag{7.4}$$

For an accurate estimate, Δl_i should be chosen small enough so that the forward and backward differences are of nearly equal value. The design procedure is outlined in the following steps:

1.) Select n speeds in the vicinity of the flutter speed

2.) Choose an appropriate Δl_i

3.) Compute $\partial\Delta E/\partial l_i$ for each speed

4.) Solve the n linear inequalities (eq. 7.3) for the components of the control law

5.) Scale the control law.

The method was applied to the airfoil analyzed in the previous section with $l=0$ ($\beta_c=0$). The root locus and -work per cycle versus velocity plots for this system are shown in figures 16 and 17 respectively. Figure 17 is the -work per cycle versus velocity plot for the plunging mode only. The plunging mode becomes unstable near 430 ft/sec. Velocities of 410, 420, 430, 440, and 450 were selected as the design speeds. The values used for Δl_i are

$\Delta l_1 = 3.333\text{x}10^{-5}$

$\Delta l_2 = 3.333\text{x}10^{-5}$

$\Delta l_3 = 1\text{x}10^{-4}$

$\Delta l_4 = 1\text{x}10^{-4}$

The set of five linear inequalities were computed as

$$
\begin{aligned}
1.4899\Delta l_1 + 0.4814\Delta l_2 + 0.4086\Delta l_3 + 0.059\Delta l_4 &< 0 \\
0.4566\Delta l_1 + 0.4078\Delta l_2 - 1.1768\Delta l_3 + 0.0586\Delta l_4 &< 0 \\
-0.5268\Delta l_1 + 0.3415\Delta l_2 - 1.2339\Delta l_3 + 0.0580\Delta l_4 &< 0 \\
-1.4518\Delta l_1 + 0.2838\Delta l_2 + 0.3708\Delta l_3 + 0.0574\Delta l_4 &< 0 \\
-2.3117\Delta l_1 + 0.2358\Delta l_2 - 1.3135\Delta l_3 + 0.0566\Delta l_4 &< 0
\end{aligned}
\tag{7.6}
$$

The solution of the set of inequalities was computed via the IMSL subroutine ZX3LP. The solution obtained from ZX3LP was scaled to the value

$$
l = [8.9004\text{X}10^{-4} \quad -1\text{X}10^{-2} \quad -3.61815\text{X}10^{-3} \quad -1\text{X}10^{-2}] \tag{7.7}
$$

The control law (eq. 7.7) was introduced into the system yielding the results shown in figures 18 and 19. Figure 19 is the -work per cycle versus velocity plot for the plunging mode only. Comparison of figures 16 and 17 with figures 18 and 19 reveals that the control law given by equation 7.7 has increased the flutter speed from 430 ft/sec to 450 ft/sec.

CONCLUSIONS

A method of control law synthesis for active flutter suppression has been developed. The method which is based upon increased energy dissipation near the flutter instability has been applied to a two-dimensional wing with a single trailing-edge control resulting in a significantly higher flutter speed. Thus the validity of this method has been established.

The control law derived from this energy method must be scaled properly due to the non-linearity of the change in Kinetic energy per cycle versus control law component change curve.

The effectiveness of geometric theory for introduction of the Kinematic control law, derived from the energy method, into the dynamical system has been demonstrated. The geometric theory was used to determine a feedback matrix f needed to construct the closed loop system matrix (A+bf).

Extension of this work should include a study of the effect on the control law elements of variations in the airfoil system geometrical, mass, and inertial parameters.

REFERENCES

1. Thompson, G. O., "Active Flutter Suppression - An Emerging Technology," Journal of Aircraft, Vol. 9, pp. 230-235, March 1972.

2. Harris, R. B. and Rickard, W. W., "Active Control Transport Design Criteria," Journal of Aircraft, Vol. 16, no. 11, pp. 737-738, Nov. 1979.

3. Doggett, R. V. and Townsend, J. L., "Flutter Suppression by Active Controls and Its Benefits," Proceedings of the SCAR Conference, NASA CP-001, 1976.

4. Abel, I.; Perry, B., III, and Murrow, H. N., "Two Synthesis Techniques Applied to Flutter Suppression on a Flight Research Wing," Journal of Guidance and Control, Vol. 1, no. 5, pp. 340-346, Sept./Oct. 1978.

5. Sandford, M. C.; Abel, I., and Gray, D., "Development and Demonstration of a Flutter-Suppression System Using Active Controls," NASA TR R-450, Dec. 1975.

6. Sevart, F. D., "Development of Active Flutter Suppression Wind Tunnel Testing Technology," AFFDL-TR-74-126, Jan. 1975.

7. Abel, I.; Newsom, J. R., and Dunn, H. J., "Application of Two Synthesis Methods for Active Flutter Suppression on an Aeroelastic Wind-Tunnel Model," AIAA paper no. 79-1633, August 1979.

8. Roger, K. L.; Hodges, G. E., and Felt, L., "Active Flutter Suppression - A Flight Test Demonstration," Journal of Aircraft, Vol. 12, no. 6, pp. 551-556, June 1975.

9. Newsom, J. R., "A Method for Obtaining Practical Flutter Suppression Control Laws Using Results of Optimal Control Theory," NASA TP-1471, 1979.

10. Nissim, E., "Flutter Suppression Using Active Controls Based on the Concept of Aerodynamic Energy," NASA TN D-6199, 1971.

11. Kussner, H. G. and Schwarz, I., "The Oscillating Wing With Aerodynamically Balanced Elevator," TM 991, Oct. 1941, NACA.

12. Edwards, J. W., "Unsteady Aerodynamic Modeling and Active Aeroelastic Control," SUDAAR 504 (NASA Grant ngl-05-020-007), Stanford Univ., Feb. 1977. (Available as NASA CR-148019.)

13. Cliff, E. M. and Lutze, F. H., "Application of Geometric Decou-

pling Theory to Synthesis of Aircraft Lateral Control Systems," Journal of Aircraft, Vol. 9, no. 11, pp. 770-776, Nov. 1972.

14. Rodden, W. P. and Stahl, B., "A Strip Method for Prediction of Damping in Subsonic Wind Tunnel and Flight Flutter Tests," Journal of Aircraft, Vol. 6, No. 1, pp. 9-17, Jan.-Feb. 1969.

Appendix A

EQUATIONS OF MOTION

The equations of motion of the airfoil section are derived using Newton's second law of motion and the moment equation for a rigid body in plane motion

$$\Sigma \vec{F}_y = m_i \vec{a}_{c.m.} \tag{A.1}$$

$$\Sigma M_{c.m.} = I_{c.m.} \dot{\omega} \tag{A.2}$$

Equations (A.1) and (A.2) are written for the main body of the airfoil (body 1) and the trailing edge control surface (body 2). All angles (α,β) are assumed to be small. The equations are linearized about the zero equilibrium ($\alpha_e=\beta_e=\dot{\alpha}_e=\dot{\beta}_e=\ddot{\alpha}_e=\ddot{\beta}_e=0$). The free body diagrams of the two bodies are shown in figures 5 and 6. Applying equations A.1 and A.2 respectively to body 1, using the small angle assumption and linearizing yields

$$K_h h - q_y + L_1 + m_1[\ddot{h} + bx_1\ddot{\alpha}] = 0 \tag{A.3}$$

$$I_Q\ddot{\alpha} + M_1 + K_\alpha\alpha - K_\beta\beta - K_h hbx_1 \quad - L_1[db - \frac{b}{2} + bx_1] - q_y[cb - bx_1] = 0 \tag{A.4}$$

Applying equations A.1 and A.2 respectively to body 2, using the small angle assumption and linearizing yields

$$q_y + L_2 + m_2[\ddot{h} + bc\ddot{\alpha} + \ell(\ddot{\beta} + \ddot{\alpha})] = 0 \tag{A.5}$$

$$-(q_y + L_2)\ell + K_\beta\beta + M_2 + I_G(\ddot{\alpha} + \ddot{\beta}) = 0 \tag{A.6}$$

Adding equations A.3 and A.5 yields the plunging equation as

$$(mb)\frac{\ddot{h}}{b} + [m_1 b x_1 + m_2(bc+\ell)]\ddot{\alpha} + m_2\ell\ddot{\beta} + (bk_h)\frac{h}{b} = -L \tag{A.7}$$

To obtain the pitching equation, equations A.3 through A.6 must be combined such that the total pitching moment about the one-quarter chord point appears in the pitching equation as

$$M = M_1 + M_2 + L_2[c+d-1/2]b \tag{A.8}$$

For the above expression to appear in the pitching equation combine equations (A.3) through (A.6) as follows

$$\mu_1(\text{eq.A.3}) + \mu_2(\text{eq.A.4}) + \mu_3(\text{eq.A.5}) + \mu_4(\text{eq.A.6})$$

where

$$\begin{aligned} \mu_1 &= (d-1/2+x_1)b \\ \mu_2 &= 1 \\ \mu_3 &= b(c+d-1/2)+\ell \\ \mu_4 &= 1 \end{aligned} \tag{A.9}$$

The above combination yields the pitching equation as

$$[m_1 b^2(d-1/2+x_1)+m_2 b^2(c+d-1/2+\frac{\ell}{b})]\frac{\ddot{h}}{b}$$

$$+[m_1 b^2 x_1(d-1/2+x_1)+I_Q+m_2 b(c+d-1/2+\frac{\ell}{b})(bc+\ell)$$

$$+I_G]\ddot{\alpha}+[m_2 b\ell(c+d-\frac{1}{2}+\frac{\ell}{b})+I_G]\ddot{\beta}$$

$$+[K_h b^2(d-1/2)]\frac{h}{b}+K_\alpha\alpha=-M \qquad \text{(A.10)}$$

The trailing edge flap equation is obtained by solving equation (A.5) for q_y and substituting into equation (A.6) as

$$(bm_2\ell)\frac{\ddot{h}}{b}+[m_2\ell(bc+\ell)+I_G]\ddot{\alpha}+(m_2\ell^2+I_G)\ddot{\beta}+K_\beta\beta=-(T+T_s) \qquad \text{(A.11)}$$

Multiplying equation (A.7) by $-b[(d+a)-1/2]$ and adding the result to equation (A.10) yields the following symmetrical matrix form for the equations of motion

$$\begin{bmatrix} bm & S_\alpha & S_\beta \\ bS_\alpha & I_\alpha & I_\beta+S_\beta bc \\ bS_\beta & I_\beta+S_\beta bc & I_\beta \end{bmatrix}\begin{bmatrix} \ddot{h}/b \\ \ddot{\alpha} \\ \ddot{\beta} \end{bmatrix}+\begin{bmatrix} bK_h & 0 & 0 \\ 0 & K_\alpha & 0 \\ 0 & 0 & K_\beta \end{bmatrix}\begin{bmatrix} h \\ \alpha \\ \beta \end{bmatrix}$$

$$=\begin{bmatrix} -L \\ -M_{e.a.} \\ -(T+T_s) \end{bmatrix} \qquad \text{(A.12)}$$

Appendix B

UNSTEADY AERODYNAMIC LOADS

The motion of the airfoil is represented by the following three degrees of freedom illustrated in figure 1

a) Plunging or bending oscillation of the entire airfoil, $z_1(x) = he^{i\omega t}$,

b) Pitching oscillation of the airfoil about the one-quarter chord point, $z_2(x) = \alpha b[x+1/2]e^{i\omega t}$,

c) Oscillation of the elevator about its leading edge or hinge line, $z_3(x) = \begin{cases} 0 & \text{for } 0 \leq \Theta \leq \varphi \\ \beta e^{i\omega t}(\cos\varphi - \cos\Theta) & \text{for } \varphi \leq \Theta \leq \pi \end{cases}$

The total wing lift, pitching moment of the total wing about the one-quarter chord point, and the elevator hinge moment about its leading edge are computed using equations 14, 16, 18, and 20 in reference 11. Equation 14 (reference 11) is rewritten as

$$\frac{\text{Total wing lift}}{\text{unit depth}} \equiv L = \pi\rho V^2 b e^{i\omega t} \quad \Sigma G K_g \tag{B.1}$$

$$\frac{\text{Total wing moment about the 1/4 chord}}{\text{unit depth}} \equiv M$$

$$= \pi\rho V^2 b^2 e^{i\omega t} \quad \Sigma G m_g \tag{B.2}$$

$$\frac{\text{Total T.E. flap hinge moment about its leading edge}}{\text{unit depth}} \equiv T$$

$$= \pi\rho V^2 b^2 e^{i\omega t} \quad \Sigma G n_g \tag{B.3}$$

where the summation is over the degrees of freedom g=a,b, and c. G represents the amplitude of degree of freedom g. Substituting in the expressions for k_a, k_b, k_c, m_a, m_b, m_c, n_a, n_b, and n_c from equations 16, 18, and 20 in reference 1, and omitting the factor $e^{i\omega t}$ for the sake of convenience, equations B.1, B.2 and B.3 become

$$L(\omega)=\pi\rho V^2 b\left\{\left\{i\left(\frac{\omega b}{V}\right)[2C(k)]-\frac{\omega^2 b^2}{V^2}\right\}\frac{h}{b}+\left\{2C(k)\left(1+i\frac{\omega b}{V}\right)\right.\right.$$

$$\left.+i\frac{\omega b}{V}-\frac{\omega^2 b^2}{2V^2}\right\}\alpha+\left\{\frac{1}{\pi}\left[2C(k)\left(\Phi_1+i\frac{\omega b}{2V}\Phi_2\right)+i\frac{\omega b}{V}\Phi_3\right.\right.$$

$$\left.\left.\left.-\frac{\omega^2 b^2}{2V^2}\Phi_4\right]\right\}\beta\right\} \tag{B.4}$$

$$M(\omega)=\pi\rho V^2 b^2\left\{-\left(\frac{\omega^2 b^2}{2V^2}\right)\frac{h}{b}+\left(i\frac{\omega b}{V}-\frac{3\omega^2 b^2}{8V^2}\right)\alpha\right.$$

$$\left.+\frac{1}{\pi}\left[\Phi_5+i\frac{\omega b}{2V}\Phi_6-\frac{\omega^2 b^2}{4V2}\Phi_7\right]\beta\right\} \tag{B.5}$$

$$T(\omega)=\pi\rho V^2 b^2\left\{\left\{\frac{1}{\pi}\left[C(k)\frac{i\omega b}{V}\Phi_8-\frac{\omega^2 b^2}{2V^2}\Phi_4\right]\right\}\frac{h}{b}\right.$$

$$+\left\{\frac{1}{\pi}\left[C(k)\left(1+i\frac{\omega b}{V}\right)\Phi_8+i\frac{\omega b}{2V}\Phi_9-\frac{\omega^2 b^2}{4V^2}\Phi_7\right]\right\}\alpha$$

$$\left.+\left\{\frac{1}{\pi^2}\left[C(k)\left(\Phi_1+i\frac{\omega b}{2V}\Phi_2\right)\Phi_8+\Phi_{10}+i\frac{\omega b}{2V}\Phi_{11}-\frac{\omega^2 b^2}{4V^2}\Phi_{12}\right]\right\}\beta\right\} \tag{B.6}$$

Equations B.4, B.5, and B.6 are rewritten below in a form similar to equations 1, 2, and 3 in reference 14.

$$L(\omega) = -\pi\rho b^2\left\{\omega^2 h + \left(\frac{\omega^2 b}{2} - i\omega V\right)\alpha - \frac{1}{\pi}\left(i\omega V\Phi_3 - \frac{\omega^2 b}{2}\Phi_4\right)\beta\right\}$$

$$-2\pi\rho V b\left[\frac{C(k)}{i\omega}\right]\left\{\omega^2 h + (\omega^2 b - i\omega V)\alpha + \frac{V}{\pi}\left(\frac{\omega^2 b}{2V}\Phi_2 - i\omega\Phi_1\right)\beta\right\} \quad \text{(B.7)}$$

$$M(\omega) = \pi\rho b^3\left\{-1/2\,\omega^2 h + \left(i\omega V - \frac{3b\omega^2}{8}\right)\alpha + \left(\frac{V^2}{\pi b}\Phi_5 + i\frac{\omega V}{2\pi}\Phi_6 - \frac{\omega^2 b}{4\pi}\Phi_7\right)\beta\right\} \quad \text{(B.8)}$$

$$T(\omega) = \pi\rho b^2\left\{-\omega^2 h\left(\frac{b}{2\pi}\Phi_4\right) + \left(i\frac{\omega b V}{2\pi}\Phi_9 - \frac{\omega^2 b^2}{4\pi}\Phi_7\right)\alpha + \left(\frac{V^2}{\pi^2}\Phi_{10} + i\frac{\omega V b}{2\pi^2}\Phi_{11} - \frac{\omega^2 b^2}{4\pi^2}\Phi_{12}\right)\beta\right\} + \pi\rho V b\left[\frac{C(k)}{i\omega}\right]$$

$$\left\{\left(-\frac{\omega^2 b}{\pi}\Phi_8\right)h + \left[\frac{Vb}{\pi}\left(i\omega - \frac{\omega^2 b}{V}\right)\Phi_8\right]\alpha + \left[\frac{Vb}{\pi^2}\left(i\omega\Phi_1 - \frac{\omega^2 b}{2V}\Phi_2\right)\Phi_8\right]\beta\right\} \quad \text{(B.9)}$$

The oscillatory loads given by equations B.7, B.8, and B.9 can be regarded as the Fourier transform of the corresponding transient loads. Thus the transient loads are the inverse Fourier transforms of the oscillatory loads. The inverse Fourier transforms of the terms containing the Theodorsen function C(k) are determined using the Convolution Theorem for Fourier transforms taking into account the fact that

the Fourier transform of the Wagner function is

$$\mathcal{F}\,\Phi\left(\frac{Vt}{b}\right) = \frac{C(k)}{i\omega} \tag{B.10}$$

Consequently the transient loads are

$$L(t) = \pi\rho b^2\left[\ddot{h} + \frac{b}{2}\ddot{\alpha} + \frac{b}{2\pi}\Phi_4\ddot{\beta} + V\dot{\alpha} + \frac{V}{\pi}\Phi_3\dot{\beta}\right]$$

$$+ 2\pi\rho VbD(t) \tag{B.11}$$

$$M(t) = \pi\rho b^3\left[\frac{1}{2}\ddot{h} + \frac{3b}{8}\ddot{\alpha} + \frac{b}{4\pi}\Phi_7\ddot{\beta} + V\dot{\alpha} + \frac{V}{2\pi}\Phi_6\dot{\beta}\right.$$

$$\left. + \frac{V^2}{\pi b}\Phi_5\beta\right] \tag{B.12}$$

$$T(t) = \pi\rho b^2\left[\left(\frac{b}{2\pi}\Phi_4\right)\ddot{h} + \left(\frac{b^2}{4\pi}\Phi_7\right)\ddot{\alpha} + \left(\frac{b^2}{4\pi^2}\Phi_{12}\right)\ddot{\beta}\right.$$

$$\left. + \left(\frac{bV}{2\pi}\Phi_9\right)\dot{\alpha} + \left(\frac{Vb}{2\pi^2}\Phi_{11}\right)\dot{\beta} + \left(\frac{V^2}{\pi^2}\Phi_{10}\right)\beta\right] + \pi\rho VbG(t) \tag{B.13}$$

where the Duhamel integrals D(t) and G(t) are

$$D(t) = \int_0^t \Phi\left[\frac{V(t-\tau)}{b}\right] Q_1'(\tau)d\tau \tag{B.14}$$

$$G(t) = \int_0^t \Phi\left[\frac{V(t-\tau)}{b}\right] Q_2'(\tau)d\tau \tag{B.15}$$

in which

$$Q_1'(\tau) = \frac{dQ_1(\tau)}{d\tau} = h'' + \alpha'' b + \frac{b}{2\pi}\Phi_2\beta'' + V\alpha' + \frac{V}{\pi}\Phi_1\beta' \tag{B.16}$$

$$Q_2'(\tau) = \frac{b}{\pi}\Phi_8 h'' + \frac{b^2}{\pi}\Phi_8\alpha'' + \frac{b^2}{2\pi^2}\Phi_2\Phi_8\beta'' + \frac{Vb}{\pi}\Phi_8\alpha'$$

$$+ \frac{Vb}{\pi^2}\Phi_1\Phi_8\beta' \tag{B.17}$$

The Duhamel integrals D(t) and G(t) are evaluated by the following expressions using the procedure outlined in reference 14.

$$D(t) = Q_1(t) - \alpha_1 B_1(t) - \alpha_2 B_2(t) \tag{B.18}$$

$$G(t) = Q_2(t) - \alpha_1 A_1(t) - \alpha_2 A_2(t) \tag{B.19}$$

α_1 and α_2 are coefficients in the two-term exponential approximation of the Wagner function suggested by W. P. Jones as

$$\Phi(Vt/b) = 1 - \alpha_1 \exp\left(-\frac{\beta_1 Vt}{b}\right) - \alpha_2 \exp\left(-\frac{\beta_2 Vt}{b}\right) \tag{B.20}$$

in which $\alpha_1 = 0.165$, $\beta_1 = 0.041$, $\alpha_2 = 0.335$, and $\beta_2 = 0.32$. The functions $B_1(t)$, $B_2(t)$, $A_1(t)$, and $A_2(t)$ are solutions of the following four first-order differential equations (see reference 14, eqs. 13, and 14)

$$\dot{B}_1 + (\beta_1 V/b)B_1 = \dot{Q}_1(t) \tag{B.21}$$

$$\dot{B}_2 + (\beta_2 V/b)B_2 = \dot{Q}_1(t) \tag{B.22}$$

$$\dot{A}_1 + (\beta_1 V/b)A_1 = \dot{Q}_2(t) \tag{B.23}$$

$$\dot{A}_2 + (\beta_2 V/b)A_2 = \dot{Q}_2(t) \tag{B.24}$$

The expressions for $Q_1(t)$ and $Q_2(t)$ are found from equations B.16 and B.17 by replacing τ by t and integrating to give

$$Q_1(t) = \dot{h} + b\dot{\alpha} + V\alpha + \frac{b}{2\pi}\Phi_2\dot{\beta} + \frac{V}{\pi}\Phi_1\beta + C_1 \tag{B.25}$$

$$Q_2(t) = (\frac{b}{\pi}\Phi_8)\dot{h} + (\frac{Vb}{\pi}\Phi_8)\alpha + (\frac{b^2}{\pi}\Phi_8)\dot{\alpha} + (\frac{Vb}{\pi^2}\Phi_1\Phi_8)\beta$$

$$+ \frac{b^2}{2\pi^2}\Phi_2\Phi_8\dot{\beta} + C_2 \tag{B.26}$$

where the arbitrary constants of integration can be set equal to zero. Combining equations B.11, B.13, B.18, B.19, B.25, and B.26 and rewriting equation B.12 the final expressions for the aerodynamic loads

$$L(t) = \pi\rho b^2\left\{[b]\frac{\ddot{h}}{b} + \left[\frac{b}{2}\right]\ddot{\alpha} + \left[\frac{b}{2\pi}\Phi_4\right]\ddot{\beta} + [2V]\frac{\dot{h}}{b} + [3V]\dot{\alpha}\right.$$

$$\left. + \frac{V}{\pi}(\Phi_3 + \Phi_2)\dot{\beta} + \left[\frac{2V^2}{b}\right]\alpha + \left[\frac{2V^2}{\pi b}\Phi_1\right]\beta - \left[\frac{2V\alpha_1}{b}\right]B_1 - \left[\frac{2V\alpha_2}{b}\right]B_2\right\}$$

$$M(t) = \pi\rho b^2\left\{\left[\frac{b^2}{2}\right]\frac{\ddot{h}}{b} + \left[\frac{3b^2}{8}\right]\ddot{\alpha} + \left[\frac{b^2}{4\pi}\Phi_7\right]\ddot{\beta} + [Vb]\dot{\alpha} + \left[\frac{Vb}{2\pi}\Phi_6\right]\dot{\beta} + \left[\frac{V^2\Phi_5}{\pi}\right]\beta\right\}$$

$$T(t) = \pi\rho b^2\left\{\left[\frac{b^2}{2\pi}\Phi_4\right]\frac{\ddot{h}}{b} + \left[\frac{b^2}{4\pi}\Phi_7\right]\ddot{\alpha} + \left[\frac{b^2}{4\pi^2}\Phi_{12}\right]\ddot{\beta} + \left[\frac{Vb}{\pi}\Phi_8\right]\frac{\dot{h}}{b}\right.$$

$$\left[\frac{Vb}{\pi}(\frac{\Phi_9}{2} + \Phi_8)\right]\dot{\alpha} + \left[\frac{Vb}{2\pi^2}(\Phi_{11} + \Phi_2\Phi_8)\right]\dot{\beta} + \left[\frac{V^2}{\pi}\Phi_8\right]\alpha + \left[\frac{V^2}{\pi^2}(\Phi_{10} + \Phi_1\Phi_8)\right]\beta$$

$$-\left[\frac{V\alpha_1}{b}\right] A_1 - \left[\frac{V\alpha_2}{b}\right] A_2 \Bigg\} \qquad \text{(B.27), (B.28), \& (B.29)}$$

Appendix C

UNSTEADY AERODYNAMIC LOADS

The aerodynamic loads acting on the airfoil section of figure 2, as derived from reference 11, involve the following functions which are dependent on the location of the flap hinge line.

$$\Phi_1 \ (\varphi) = \pi - \varphi + \sin\varphi$$

$$\Phi_2 \ (\varphi) = (\pi - \varphi)\ (1 + 2\cos\varphi) + \sin\varphi\,(2 + \cos\varphi)$$

$$\Phi_3 \ (\varphi) = \pi - \varphi + \sin\varphi\cos\varphi$$

$$\Phi_4 \ (\varphi) = (\pi - \varphi) \cdot 2\cos\varphi + \sin\varphi \cdot \frac{2}{3}(2 + \cos^2\varphi)$$

$$\Phi_5 \ (\varphi) = \sin\varphi\,(1 - \cos\varphi)$$

$$\Phi_6 \ (\varphi) = 2(\pi - \varphi) + \sin\varphi \cdot \frac{2}{3}(2 - \cos\varphi)\ (1 + 2\cos\varphi)$$

$$\Phi_7 \ (\varphi) = (\pi - \varphi)\ (\tfrac{1}{2} + 2\cos\varphi) + \sin\varphi \cdot \frac{1}{6}(8 + 5\cos\varphi + 4\cos^2\varphi - 2\cos^3\varphi)$$

$$\Phi_8 \ (\varphi) = (\pi - \varphi)\ (-1 + 2\cos\varphi) + \sin\varphi\,(2 - \cos\varphi)$$

$$\Phi_9 \ (\varphi) = (\pi - \varphi)\ (1 + 2\cos\varphi) + \sin\varphi \cdot \frac{1}{3}(2 + 3\cos\varphi + 4\cos^2\varphi)$$

$$\Phi_{10} \ (\varphi) = \Phi_{31}\ (\varphi) \cdot \Phi_5\ (\varphi)$$

$$\Phi_{11} \ (\varphi) = \Phi_2\ (\varphi) \cdot \Phi_3\ (\varphi)$$

$$\Phi_{12} \ (\varphi) = (\pi - \varphi)^2 (\tfrac{1}{2} + 4\cos^2\varphi) + (\pi - \varphi)\ \sin\varphi\cos\varphi \cdot (7 + 2\cos^2\varphi) + \sin^2\varphi\,(2 + \tfrac{5}{2}\cos^2\varphi)$$

Appendix D

STATE SPACE EQUATIONS OF MOTION

The airfoil section equations of motion (open loop; $T_s=0$) are transformed into the state space representation (eq. 3.2) in this appendix.

Combine equations A.7, A.10, and A.11 as

$$M\ddot{Y} + KY = -\begin{bmatrix} L \\ M \\ T \end{bmatrix} \tag{D.1}$$

where the unsteady aerodynamic loads L, M, and T given by equations B.27, B.28, and B.29 are written as

$$L = \pi\rho b^2 \left\{ [L_{\ddot{h}}\ L_{\ddot{\alpha}}\ L_{\ddot{\beta}}] \begin{bmatrix} \ddot{h}/b \\ \ddot{\alpha} \\ \ddot{\beta} \end{bmatrix} + [L_{\dot{h}}\ L_{\dot{\alpha}}\ L_{\dot{\beta}}] \begin{bmatrix} \dot{h}/b \\ \dot{\alpha} \\ \dot{\beta} \end{bmatrix} + [0\ L_{\alpha}\ L_{\beta}] \begin{bmatrix} h/b \\ \alpha \\ \beta \end{bmatrix} + [L_{B_1} L_{B_2}\ 0\ 0] \begin{bmatrix} B_1 \\ B_2 \\ A_1 \\ A_2 \end{bmatrix} \right\} \tag{D.2}$$

$$M = \pi\rho b^2 \left\{ [M_{\ddot{h}}\ M_{\ddot{\alpha}}\ M_{\ddot{\beta}}] \begin{bmatrix} \ddot{h}/b \\ \ddot{\alpha} \\ \ddot{\beta} \end{bmatrix} + [0\ M_{\dot{\alpha}}\ M_{\dot{\beta}}] \begin{bmatrix} \dot{h}/b \\ \dot{\alpha} \\ \dot{\beta} \end{bmatrix} + [0\ 0\ M_{\beta}] \begin{bmatrix} h/b \\ \alpha \\ \beta \end{bmatrix} \right\} \tag{D.3}$$

$$T = \pi\rho b^2 \left\{ [T_{\ddot{h}} T_{\ddot{\alpha}} T_{\ddot{\beta}}] \begin{bmatrix} \ddot{\frac{h}{b}} \\ \ddot{\alpha} \\ \ddot{\beta} \end{bmatrix} + [T_{\dot{h}} T_{\dot{\alpha}} T_{\dot{\beta}}] \begin{bmatrix} \dot{\frac{h}{b}} \\ \dot{\alpha} \\ \dot{\beta} \end{bmatrix} + [0 \;\; T_{\alpha} T_{\beta}] \begin{bmatrix} \frac{h}{b} \\ \alpha \\ \beta \end{bmatrix} \right.$$

$$\left. + [0 \;\; 0 \;\; T_{A_1} \;\; T_{A_2}] \begin{bmatrix} B_1 \\ B_2 \\ A_1 \\ A_2 \end{bmatrix} \right\} \tag{D.4}$$

Rewrite equation D.1 as

$$M'\ddot{Y} + K'Y = -\pi\rho b^2 [Z_1 \ddot{Y} + Z_2 \dot{Y} + Z_3 Y + Z_4 x_A] \tag{D.5}$$

where

$$Z_1 = \begin{bmatrix} L_{\ddot{h}} & L_{\ddot{\alpha}} & L_{\ddot{\beta}} \\ M_{\ddot{h}} & M_{\ddot{\alpha}} & M_{\ddot{\beta}} \\ T_{\ddot{h}} & T_{\ddot{\alpha}} & T_{\ddot{\beta}} \end{bmatrix} , \qquad Z_2 = \begin{bmatrix} L_{\dot{h}} & L_{\dot{\alpha}} & L_{\dot{\beta}} \\ 0 & M_{\dot{\alpha}} & M_{\dot{\beta}} \\ T_{\dot{h}} & T_{\dot{\alpha}} & T_{\dot{\beta}} \end{bmatrix} ,$$

$$Z_3 = \begin{bmatrix} 0 & L_{\alpha} & L_{\beta} \\ 0 & 0 & M_{\beta} \\ 0 & T_{\alpha} & T_{\beta} \end{bmatrix} , \qquad Z_4 = \begin{bmatrix} L_{B_1} & L_{B_2} & 0 & 0 \\ 0 & 0 & 0 & 0 \\ 0 & 0 & T_{A_1} & T_{A_2} \end{bmatrix} \tag{D.6}$$

Solving equation D.5 for $\ddot{Y}$ gives

$$\ddot{Y} = -[M' + \pi\rho b^2 Z_1]^{-1} \; [\pi\rho b^2 \; Z_2 \dot{Y} + (K' + \pi\rho b^2 Z_3) Y + \pi\rho b^2 Z_4 x_A] \tag{D.7}$$

Rewrite equations B.16 and B.17 as

$$\dot{Q}_1 = [R_1 \;\; R_2 \;\; R_3] \begin{bmatrix} \ddot{\frac{h}{b}} \\ \ddot{\alpha} \\ \ddot{\beta} \end{bmatrix} + [0 \;\; R_4 \;\; R_5] \begin{bmatrix} \dot{\frac{h}{b}} \\ \dot{\alpha} \\ \dot{\beta} \end{bmatrix} \tag{D.8}$$

$$\dot{Q}_2 = [R_6 \;\; R_7 \;\; R_8] \begin{bmatrix} \ddot{\frac{h}{b}} \\ \ddot{\alpha} \\ \ddot{\beta} \end{bmatrix} + [0 \;\; R_9 \;\; R_{10}] \begin{bmatrix} \dot{\frac{h}{b}} \\ \dot{\alpha} \\ \dot{\beta} \end{bmatrix} \tag{D.9}$$

Referring to equation 3.2 and substituting for $\ddot{Y}$ in terms of $\dot{Y}$, Y, and x_A equations D.8 and D.9 become

$$\dot{Q}_1 = [R_1\ R_2\ R_3]\left\{A_{11}\begin{bmatrix}\dot{\frac{h}{b}}\\ \dot{\alpha}\\ \dot{\beta}\end{bmatrix} + A_{12}\begin{bmatrix}\frac{h}{b}\\ \alpha\\ \beta\end{bmatrix} + A_{13}\begin{bmatrix}B_1\\ B_2\\ A_1\\ A_2\end{bmatrix}\right\} + [0\ R_4\ R_5]\begin{bmatrix}\dot{\frac{h}{b}}\\ \dot{\alpha}\\ \dot{\beta}\end{bmatrix} \tag{D.10}$$

$$\dot{Q}_2 = [R_6\ R_7\ R_8]\left\{A_{11}\begin{bmatrix}\dot{\frac{h}{b}}\\ \dot{\alpha}\\ \dot{\beta}\end{bmatrix} + A_{12}\begin{bmatrix}\frac{h}{b}\\ \alpha\\ \beta\end{bmatrix} + A_{13}\begin{bmatrix}B_1\\ B_2\\ A_1\\ A_2\end{bmatrix}\right\} + [0\ R_9\ R_{10}]\begin{bmatrix}\dot{\frac{h}{b}}\\ \dot{\alpha}\\ \dot{\beta}\end{bmatrix} \tag{D.11}$$

Rewrite equations B.21 through B.24 as

$$\begin{bmatrix}\dot{B}_1\\ \dot{B}_2\\ \dot{A}_1\\ \dot{A}_2\end{bmatrix} = \begin{bmatrix}-\frac{\beta_1 V}{b} & 0 & 0 & 0\\ 0 & -\frac{\beta_2 V}{b} & 0 & 0\\ 0 & 0 & -\frac{\beta_1 V}{b} & 0\\ 0 & 0 & 0 & -\frac{\beta_2 V}{b}\end{bmatrix}\begin{bmatrix}B_1\\ B_2\\ A_1\\ A_2\end{bmatrix} + \begin{bmatrix}\dot{Q}_1\\ \dot{Q}_1\\ \dot{Q}_2\\ \dot{Q}_2\end{bmatrix} \tag{D.12}$$

Referring to equation D.7 the A_{11}, A_{12}, and A_{13} matrices are

$$\begin{aligned} A_{11} &= -[M' + \pi\rho b^2 Z_1]^{-1}\ \pi\rho b^2 Z_2 \\ A_{12} &= -[M' + \pi\rho b^2 Z_1]^{-1}\ (K' + \pi\rho b^2 Z_3) \\ A_{13} &= -[M' + \pi\rho b^2 Z_1]^{-1}\ \pi\rho b^2 Z_4 \end{aligned} \tag{D.13}$$

The A_{21}, A_{22}, and A_{23} matrices are

$$A_{21} = \begin{bmatrix} 1 & 0 & 0 \\ 0 & 1 & 0 \\ 0 & 0 & 1 \end{bmatrix}, \quad A_{22} = \begin{bmatrix} 0 & 0 & 0 \\ 0 & 0 & 0 \\ 0 & 0 & 0 \end{bmatrix}, \quad A_{23} = \begin{bmatrix} 0 & 0 & 0 \\ 0 & 0 & 0 \\ 0 & 0 & 0 \end{bmatrix} \tag{D.14}$$

Referring to equations D.10, D.11, and D.12 the A_{31}, A_{32} and A_{33} matrices are

$$A_{31} = \begin{bmatrix} [R_1 \ R_2 \ R_3]A_{11} + [0 \ R_4 \ R_5] \\ [R_1 \ R_2 \ R_3]A_{11} + [0 \ R_4 \ R_5] \\ [R_6 \ R_7 \ R_8]A_{11} + [0 \ R_9 \ R_{10}] \\ [R_6 \ R_7 \ R_9]A_{11} + [0 \ R_9 \ R_{10}] \end{bmatrix} \tag{D.15}$$

$$A_{32} = \begin{bmatrix} [R_1 \ R_2 \ R_3] \ A_{12} \\ [R_1 \ R_2 \ R_3] \ A_{12} \\ [R_6 \ R_7 \ R_8] \ A_{12} \\ [R_6 \ R_7 \ R_8] \ A_{12} \end{bmatrix} \tag{D.16}$$

$$A_{33} = \begin{bmatrix} \begin{bmatrix} -\frac{\beta_1 V}{b} & 0 & 0 & 0 \\ 0 & -\frac{\beta_2 V}{b} & 0 & 0 \\ 0 & 0 & -\frac{\beta_1 V}{b} & 0 \\ 0 & 0 & 0 & -\frac{\beta_2 V}{b} \end{bmatrix} + \begin{matrix} [R_1 \ R_2 \ R_3] \\ [R_1 \ R_2 \ R_3] \\ [R_6 \ R_7 \ R_8] \\ [R_6 \ R_7 \ R_8] \end{matrix} \end{bmatrix} \tag{D.17}$$

Table 1. The Parameters for Edward's Three-Degree-of-Freedom Airfoil

m	$= 2.6883 \frac{\text{slugs}}{\text{ft.}}$	I_α	$= 6.04868 \frac{\text{slug-ft.}^2}{\text{ft.}}$
b	$= 3$ ft.		
S_α	$= 1.61298$ slugs	I_β	$= 0.151217 \frac{\text{slug-ft.}^2}{\text{ft.}}$
S_β	$= 0.10081$ slug	c	$= 1.0$

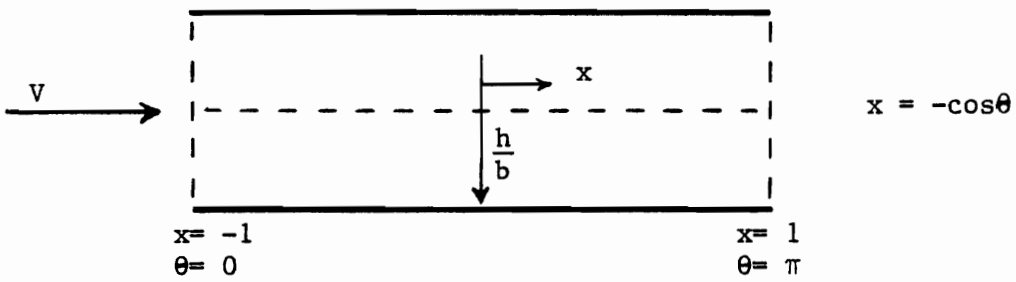

Figure 1(a). The Plunging Oscillation of the Total Wing.

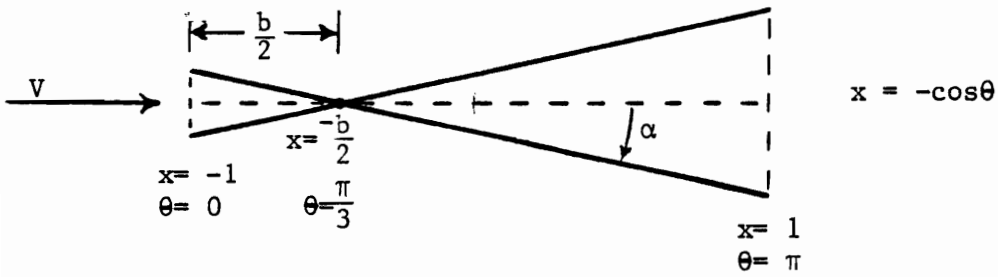

Figure 1(b). The Pitching Oscillation of the Wing about the One-Quarter Chord Point.

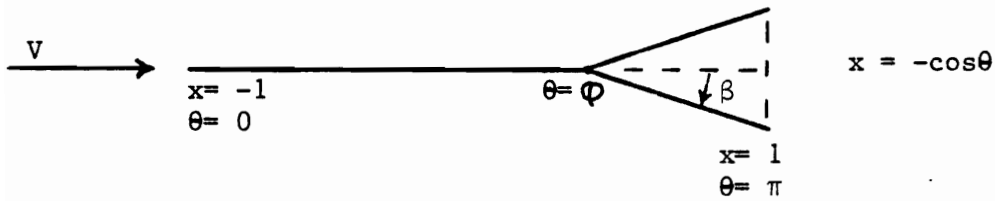

Figure 1(c). The Oscillation of the Elevator about its Leading Edge.

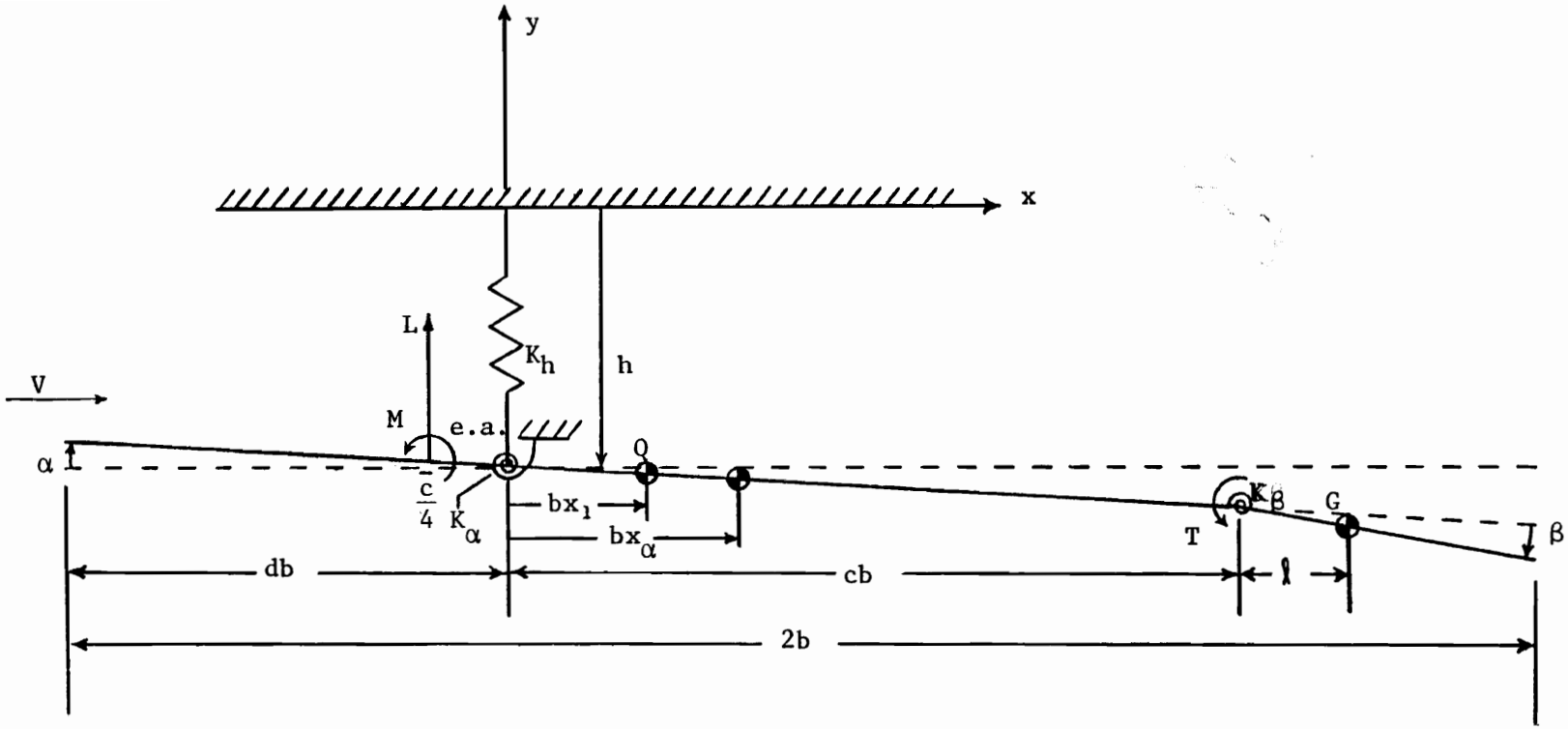

Figure 2. Diagram of a Typical Section with Aerodynamically Unbalanced Trailing-Edge Flap.

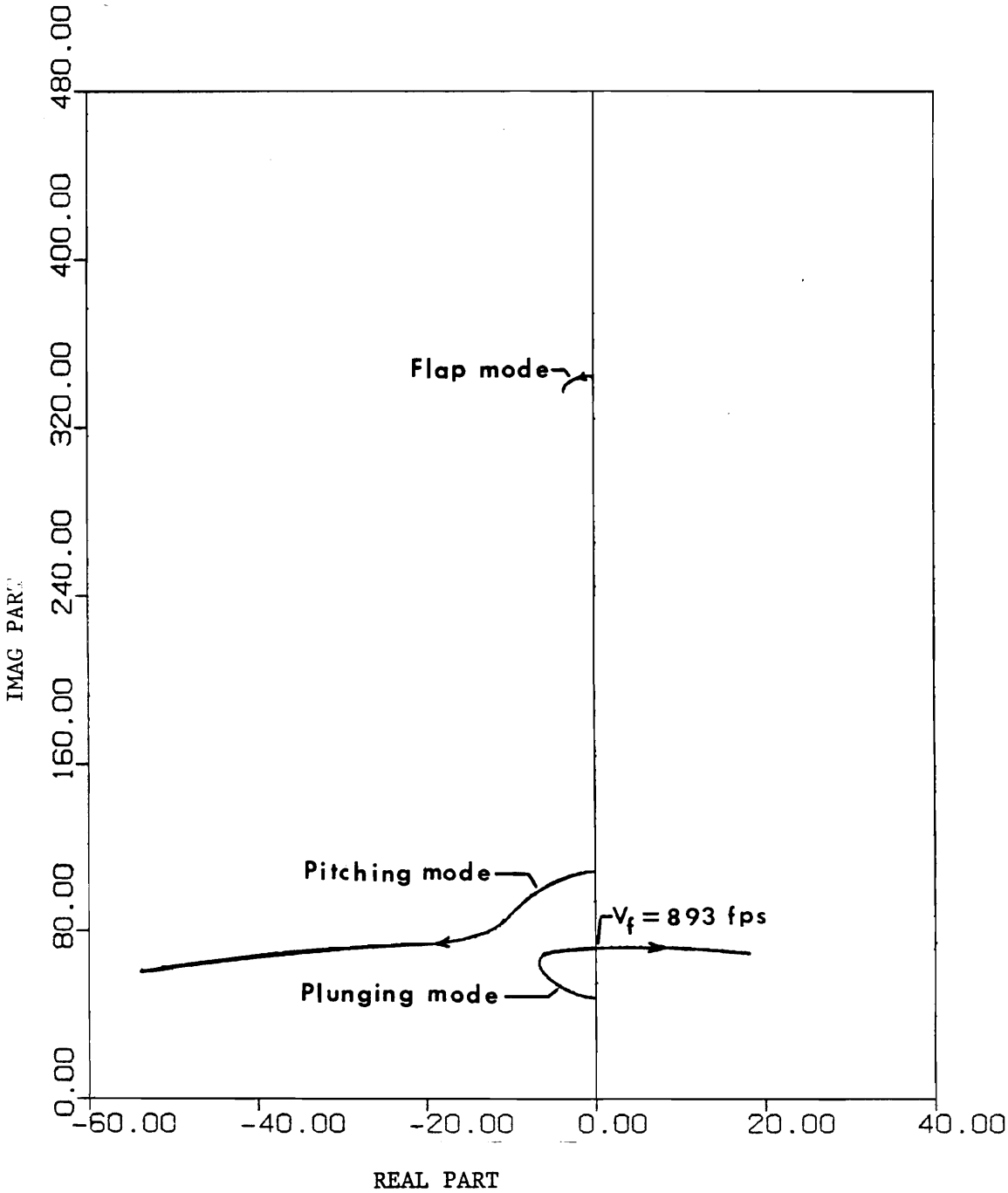

Figure 3. Root Locus for the Edward's Three-Degree-of-Freedom Airfoil

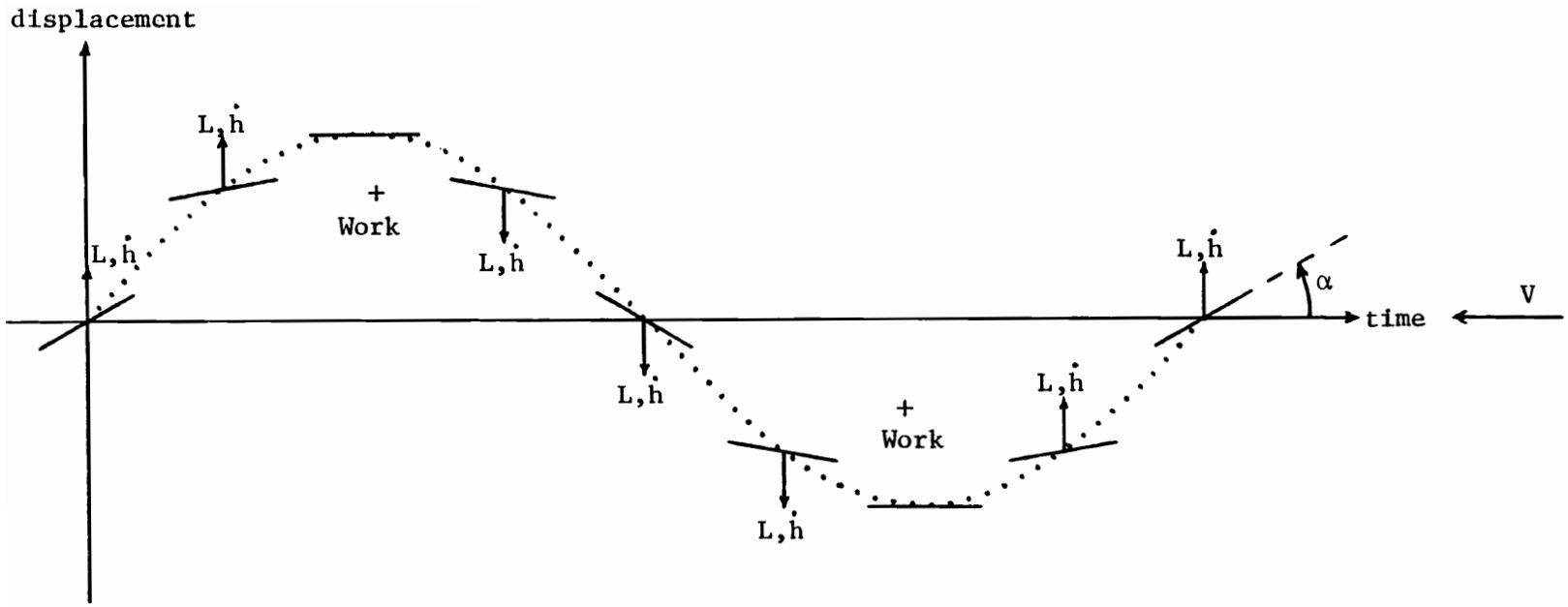

Figure 4. Motion Phasing Characteristic of Flutter

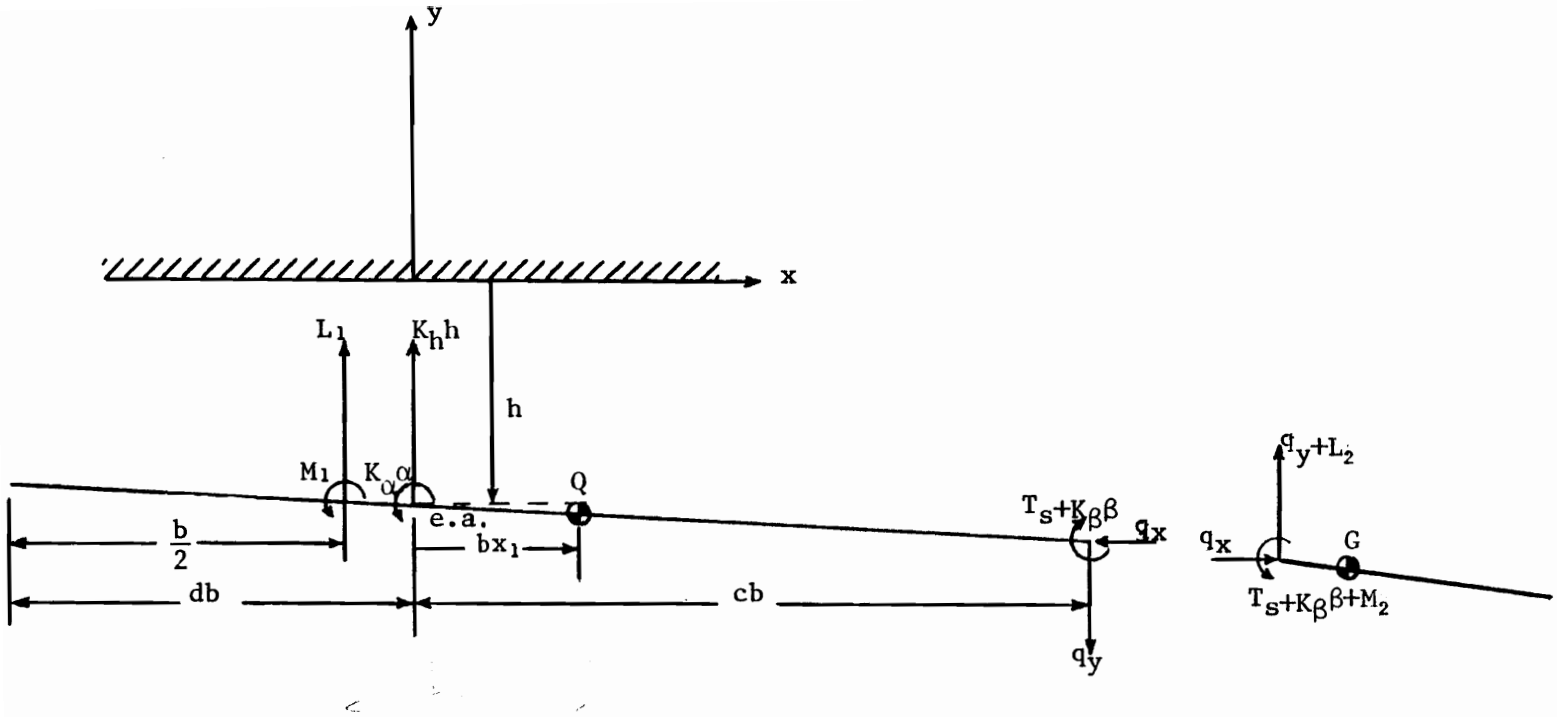

Figure 5. Free Body Diagram of a Typical Section with Aerodynamically Unbalanced Trailing Edge Flap.

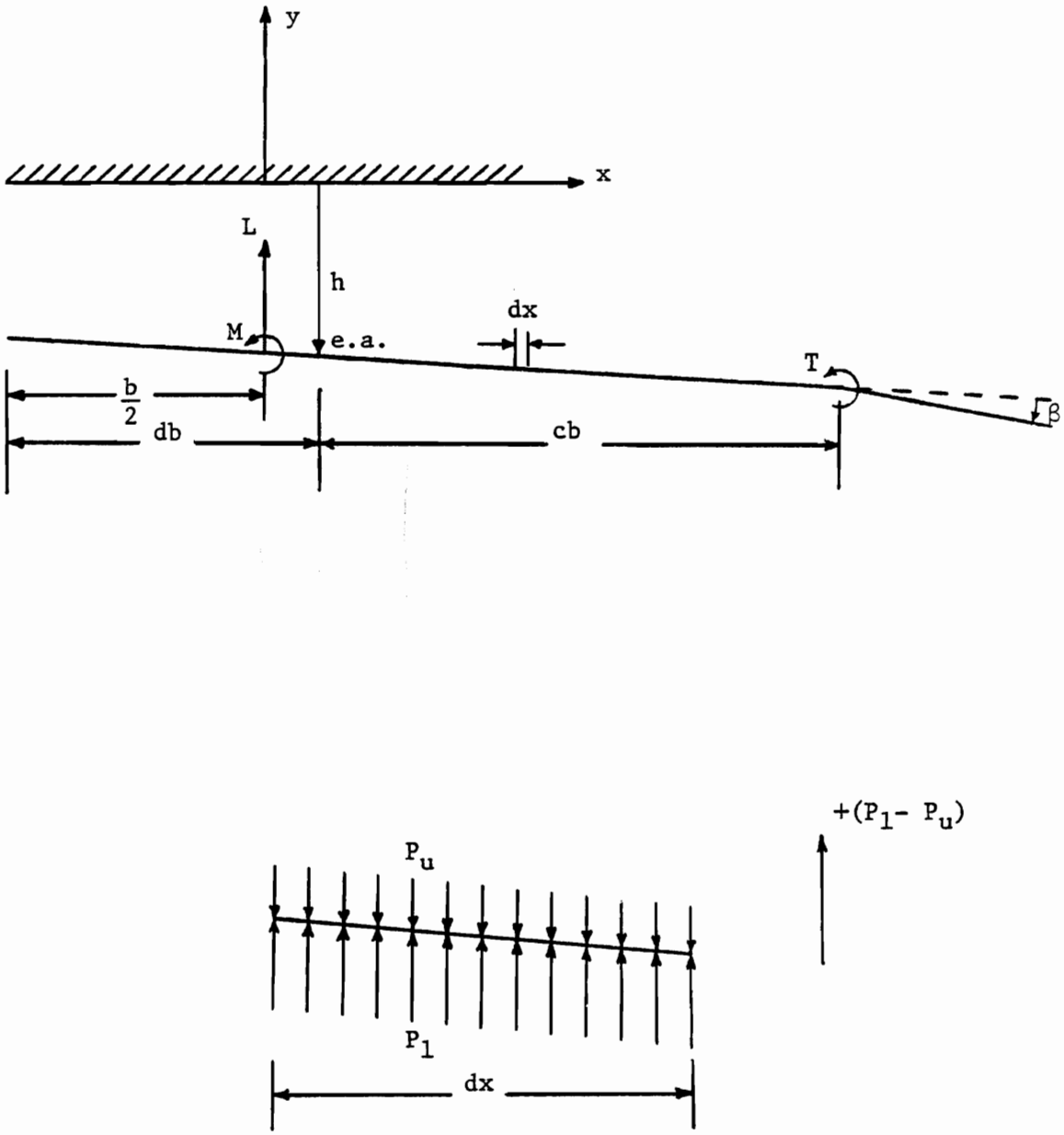

Figure 6. Airfoil Coordinate System and Aerodynamic Load Representation for the Energy Flow Analysis.

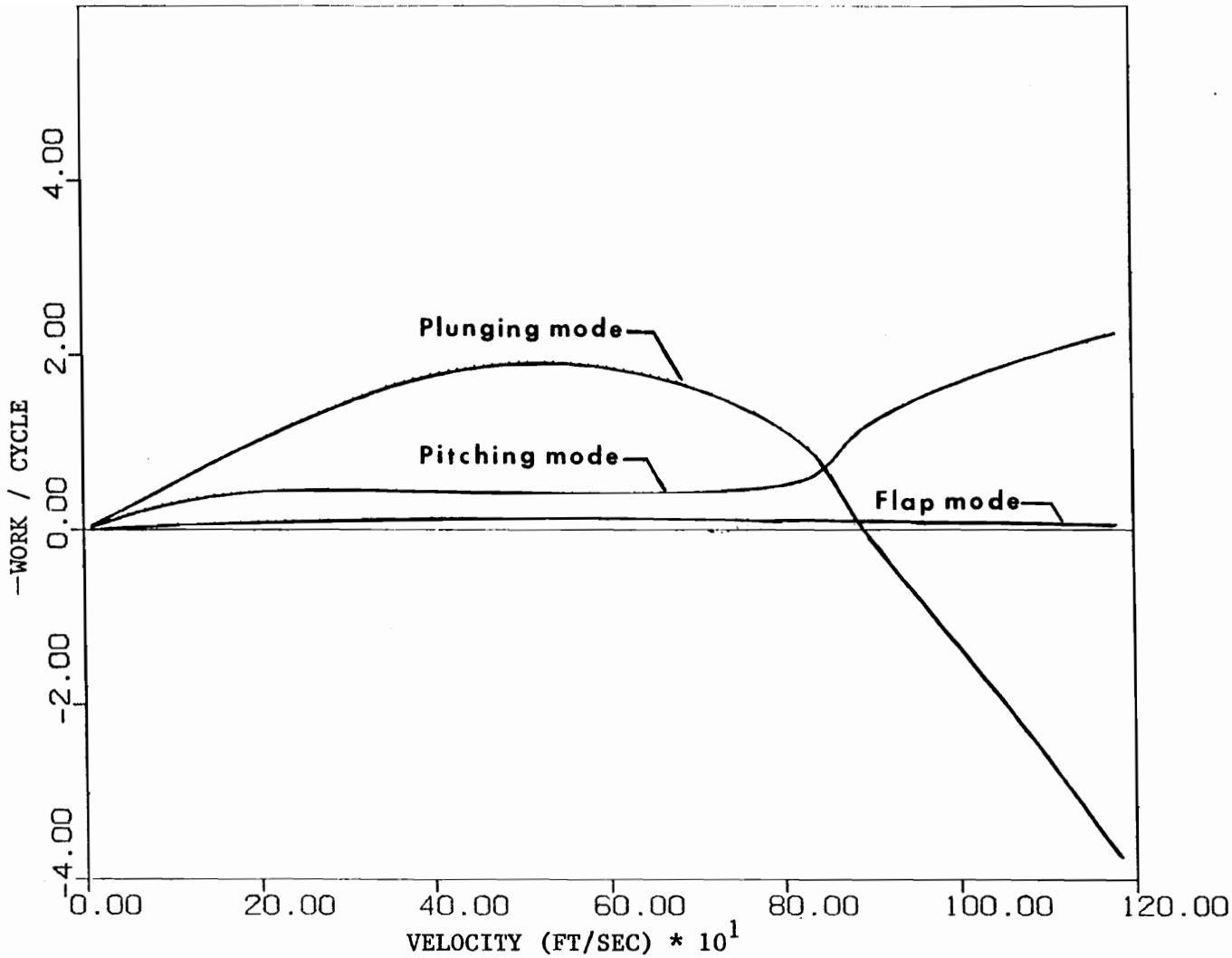

Figure 7. Work Per Cycle for the Edward's Three-Degree-of-Freedom Airfoil Case.

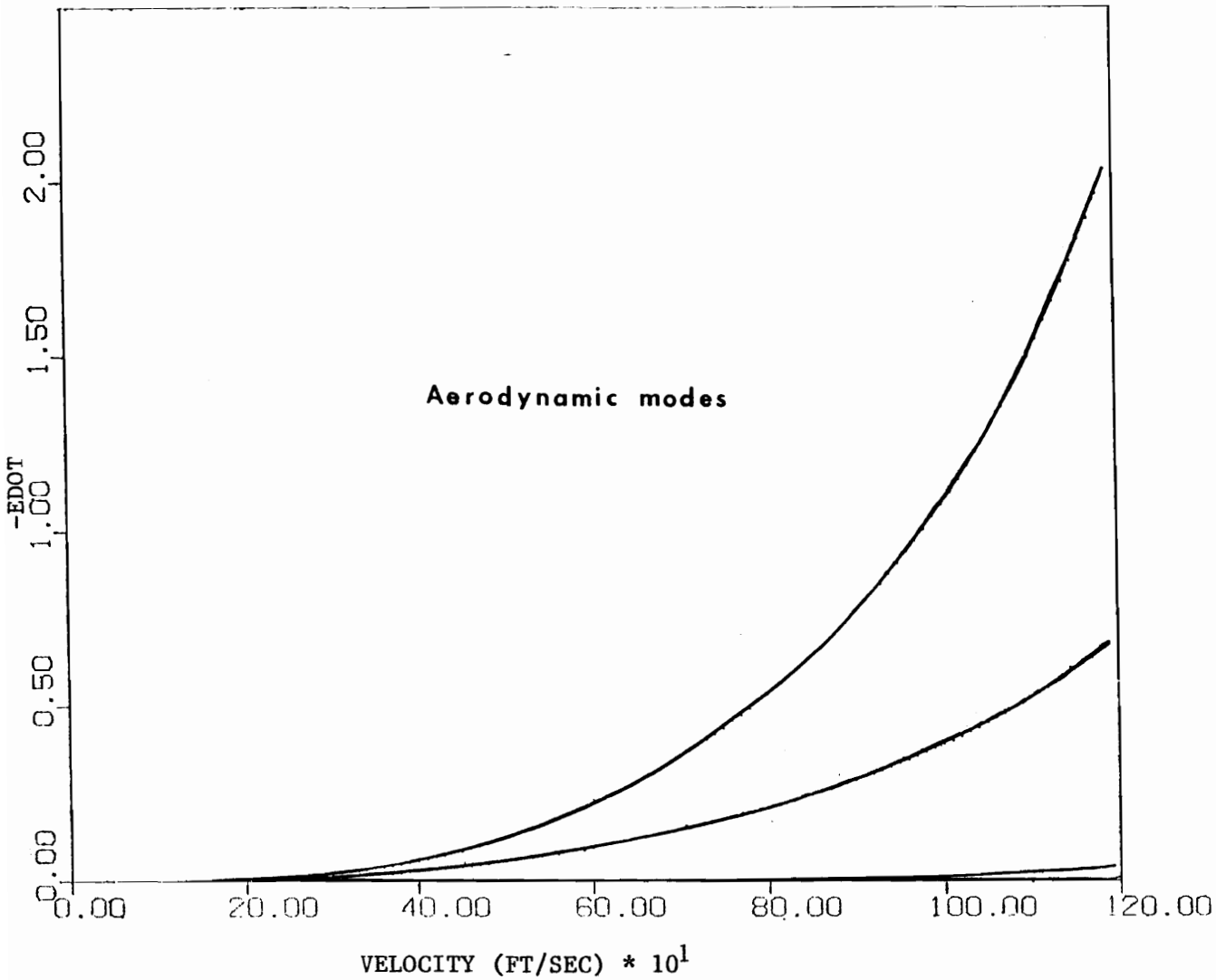

Figure 8. Instantaneous Energy Flow for the Edward's Three-Degree-of-Freedom Airfoil Case.

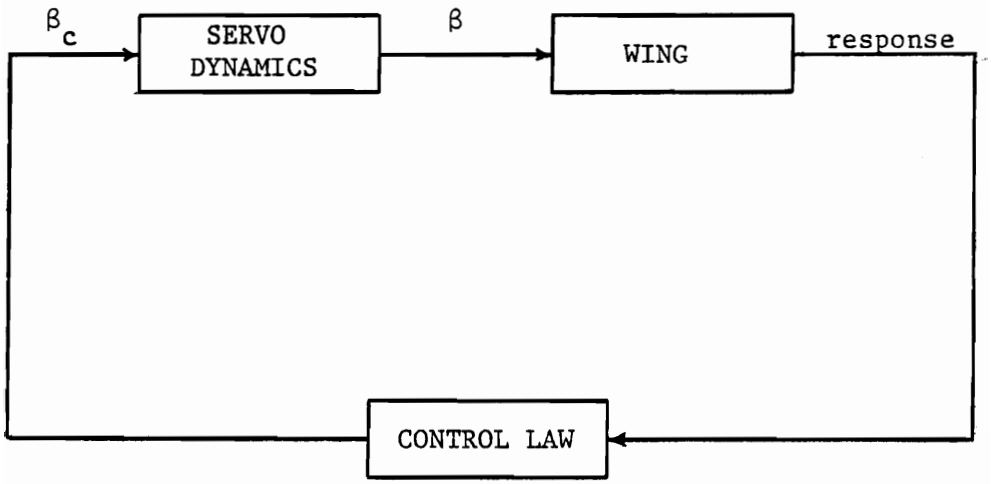

Figure 9. Block Diagram of a Flutter Suppression System

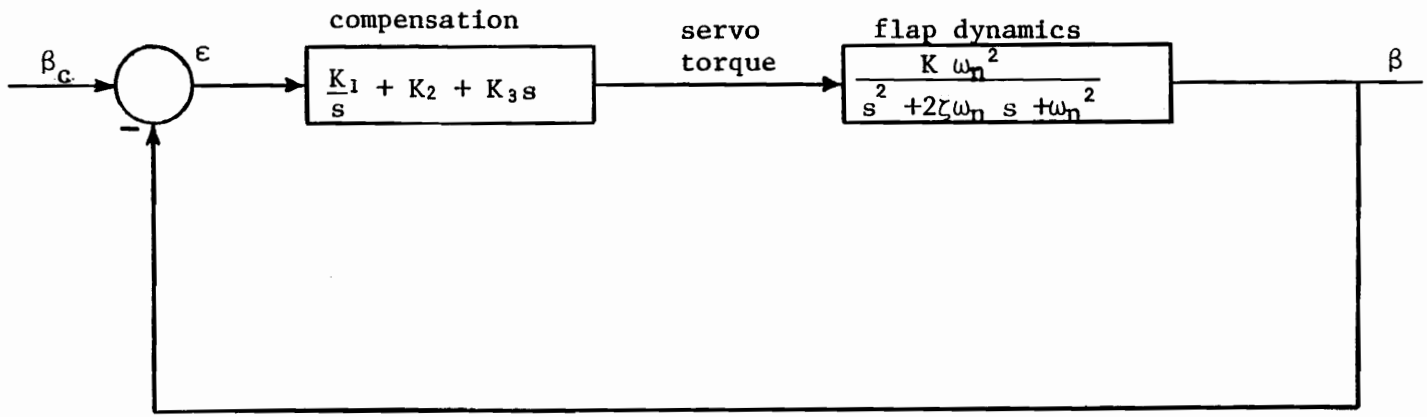

Figure 10. Block Diagram of Flap Servomechanism

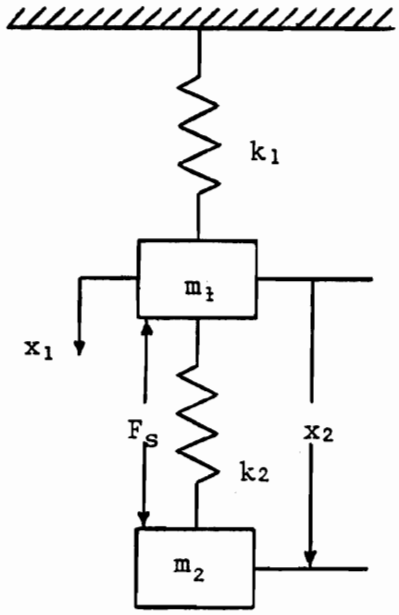

Figure 11. Two-Degree-of-Freedom Mass-Spring System.

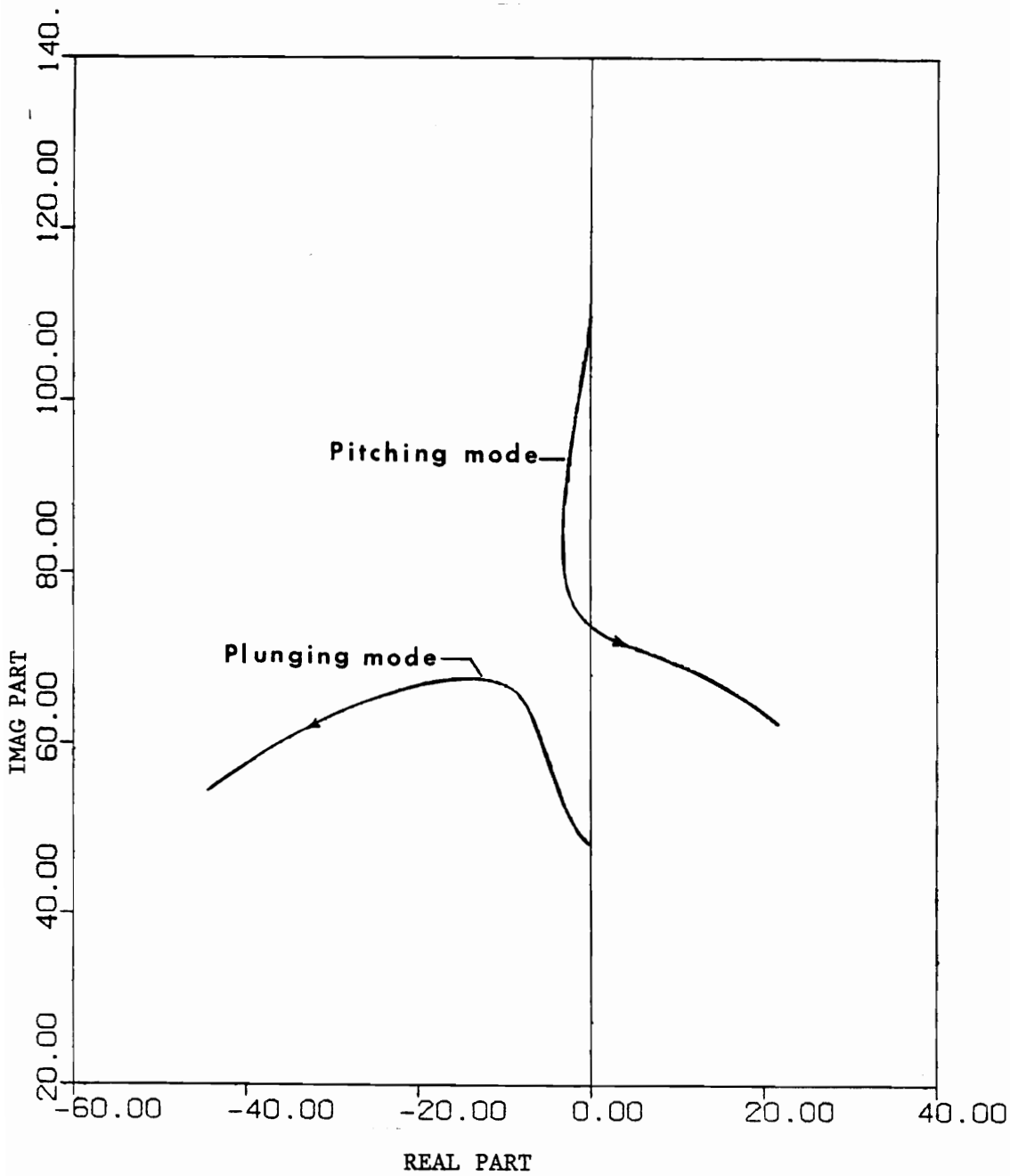

Figure 12. Root Locus for the Open Loop, Zero Flap Inertia Airfoil Case.

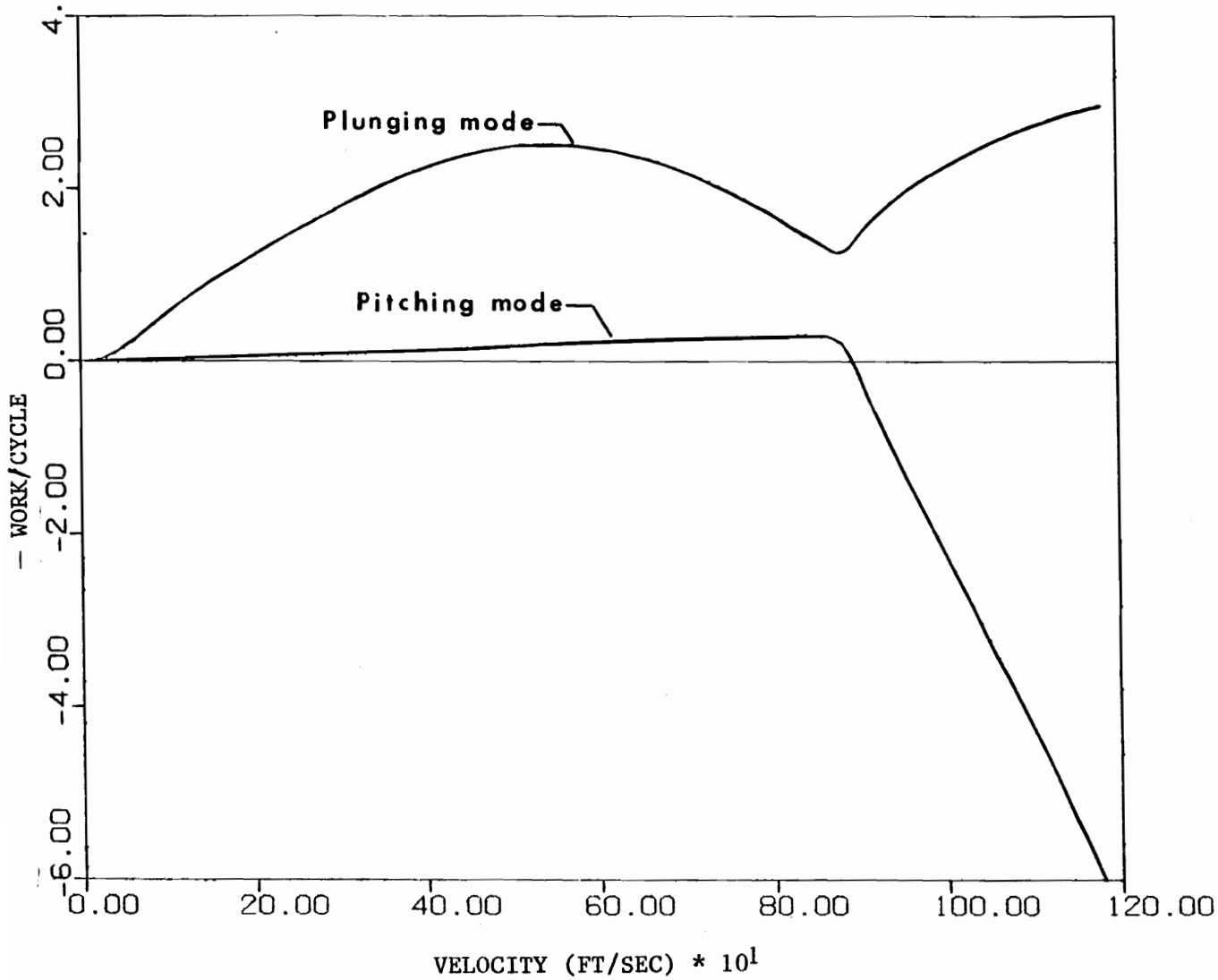

Figure 13. Work Per Cycle for the Open Loop, Zero Flap Inertia Airfoil Case.

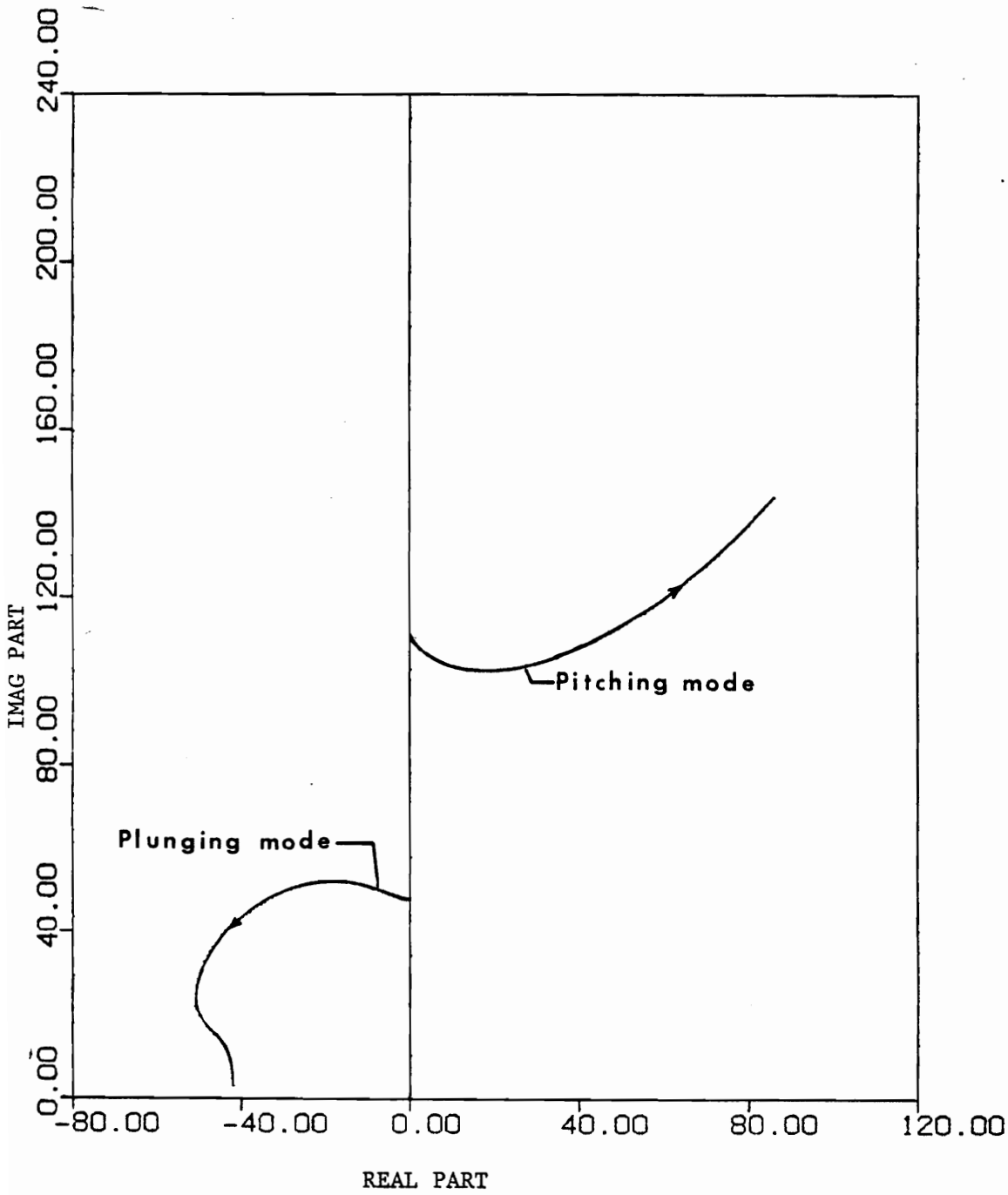

Figure 14. Root Locus for the Nissim Control Law, Zero Flap Inertia Airfoil Case.

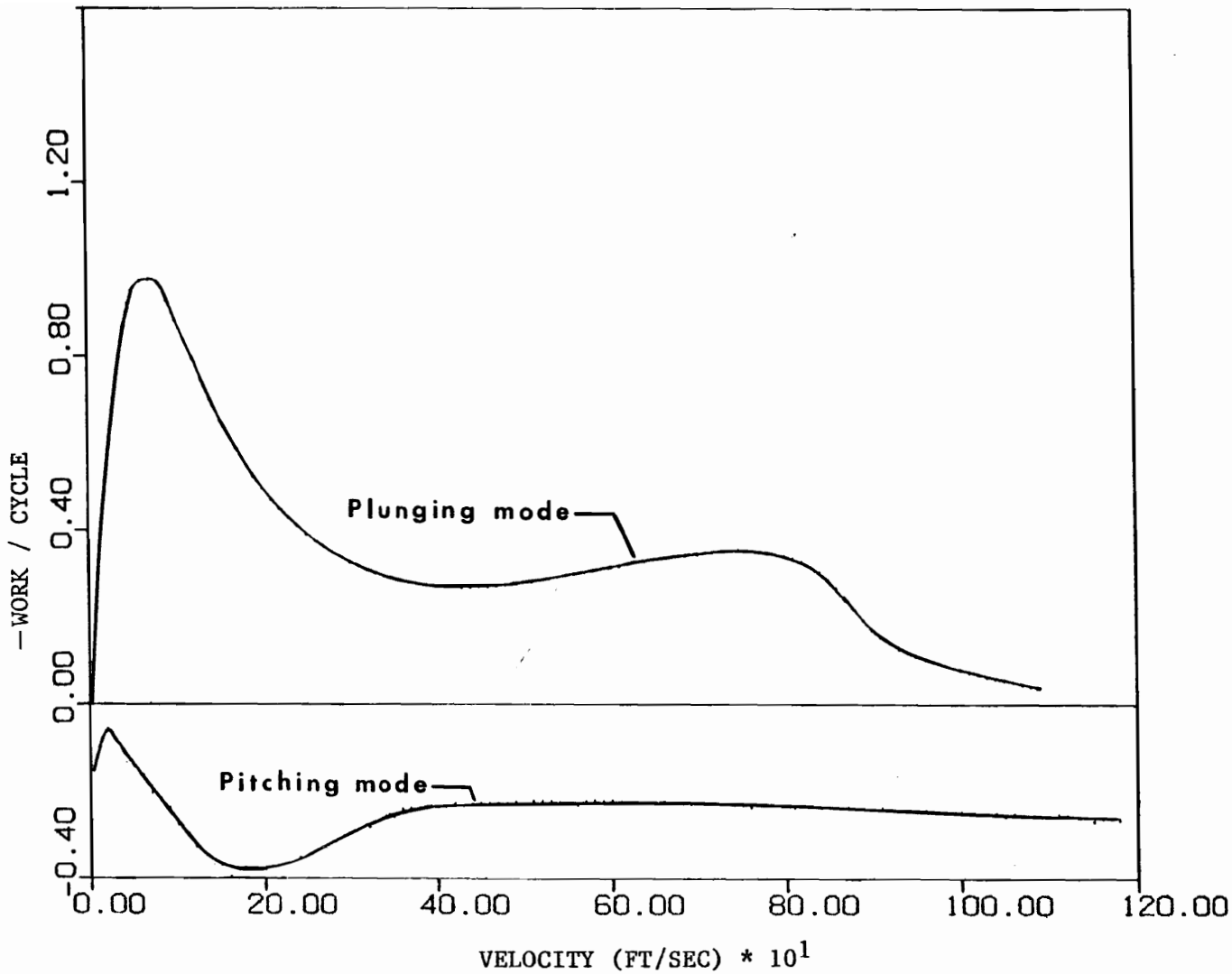

Figure 15. Work Per Cycle for the Nissim Control Law, Zero Flap Inertia Airfoil Case.

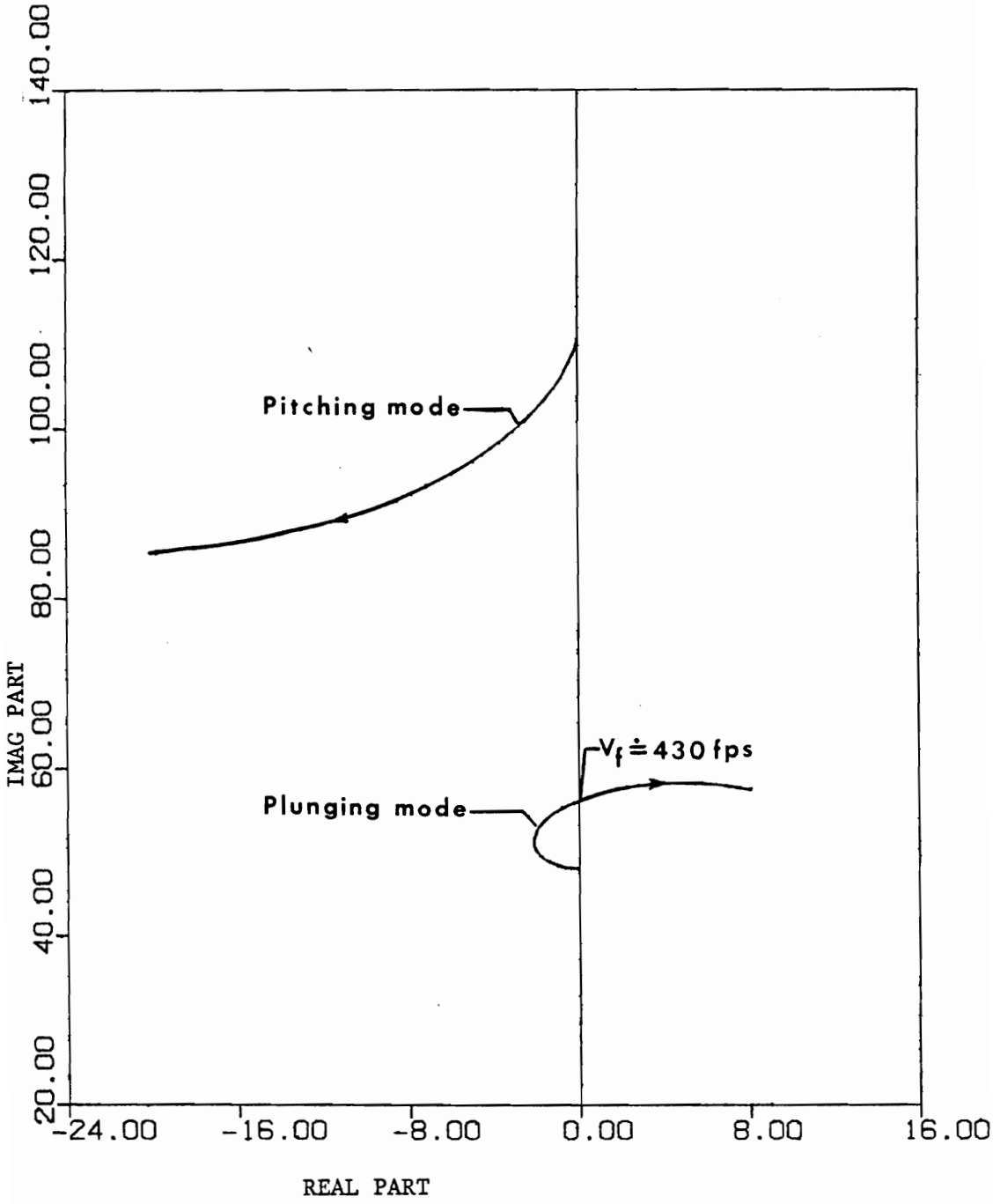

Figure 16. Root Locus for the $\beta_c = 0$, Zero Flap Inertia Case.

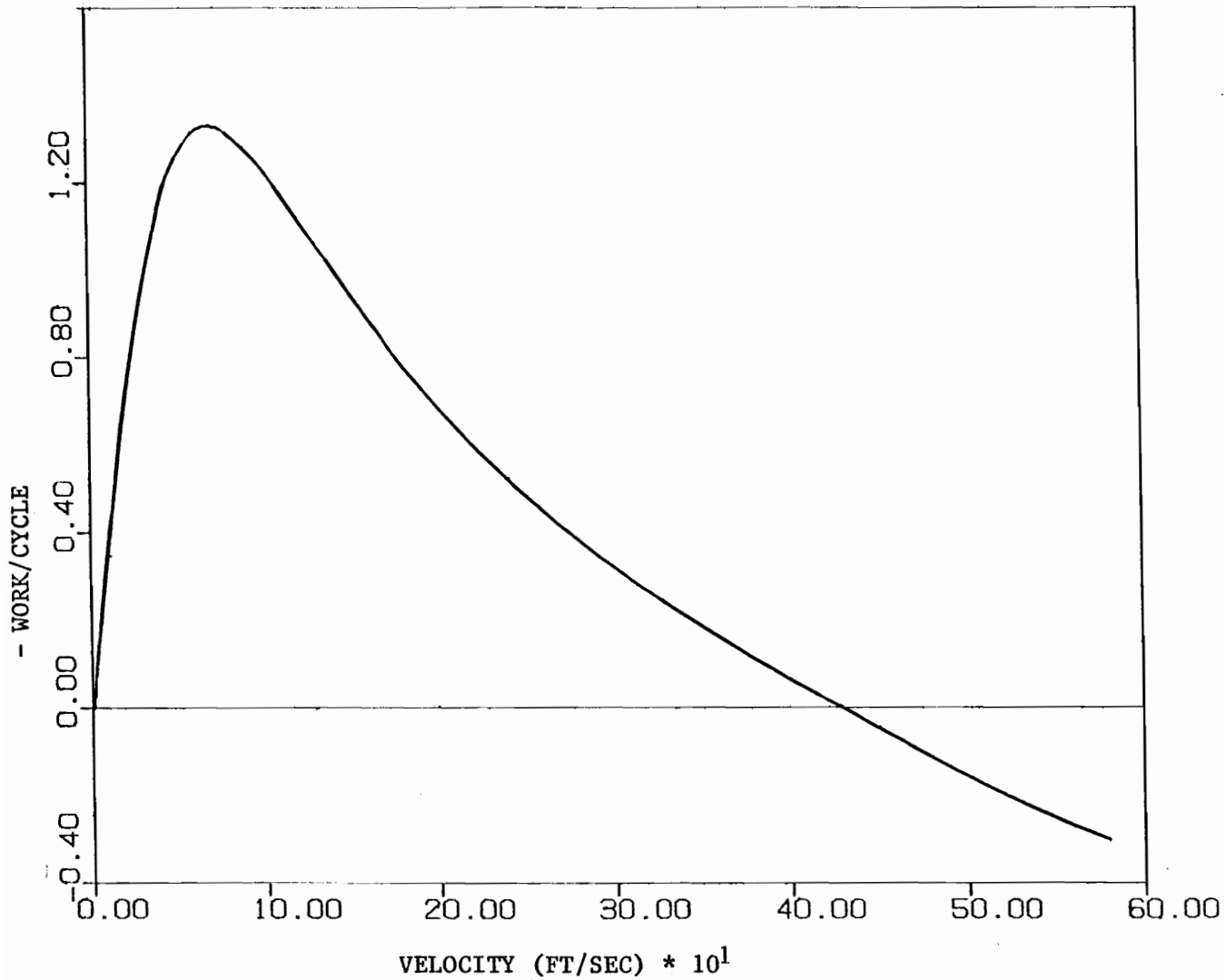

Figure 17. Work Per Cycle for the $\beta_c = 0$, Zero Flap Inertia Case.

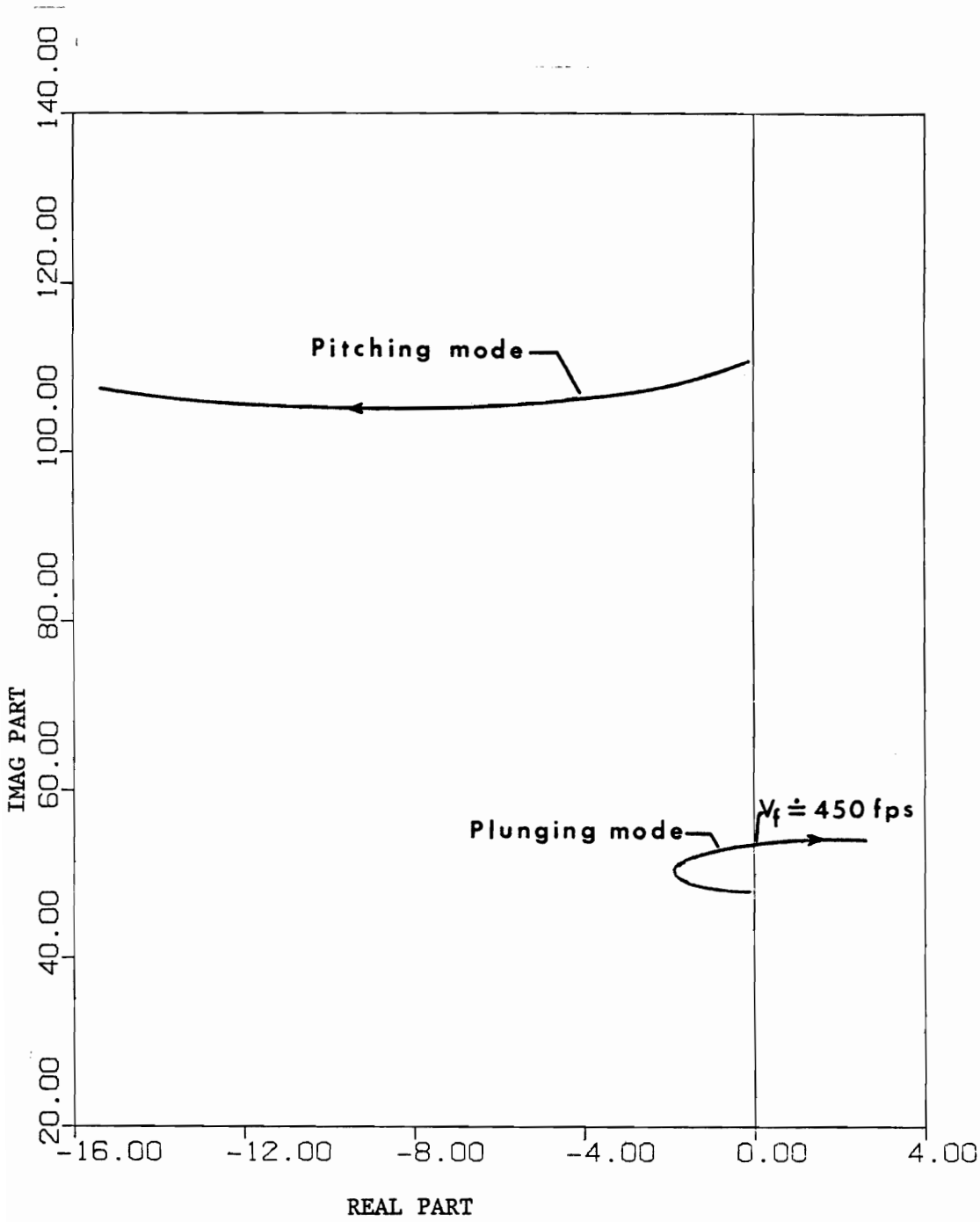

Figure 18. Root Locus for the Synthesized Control Law, Zero Flap Inertia Case.

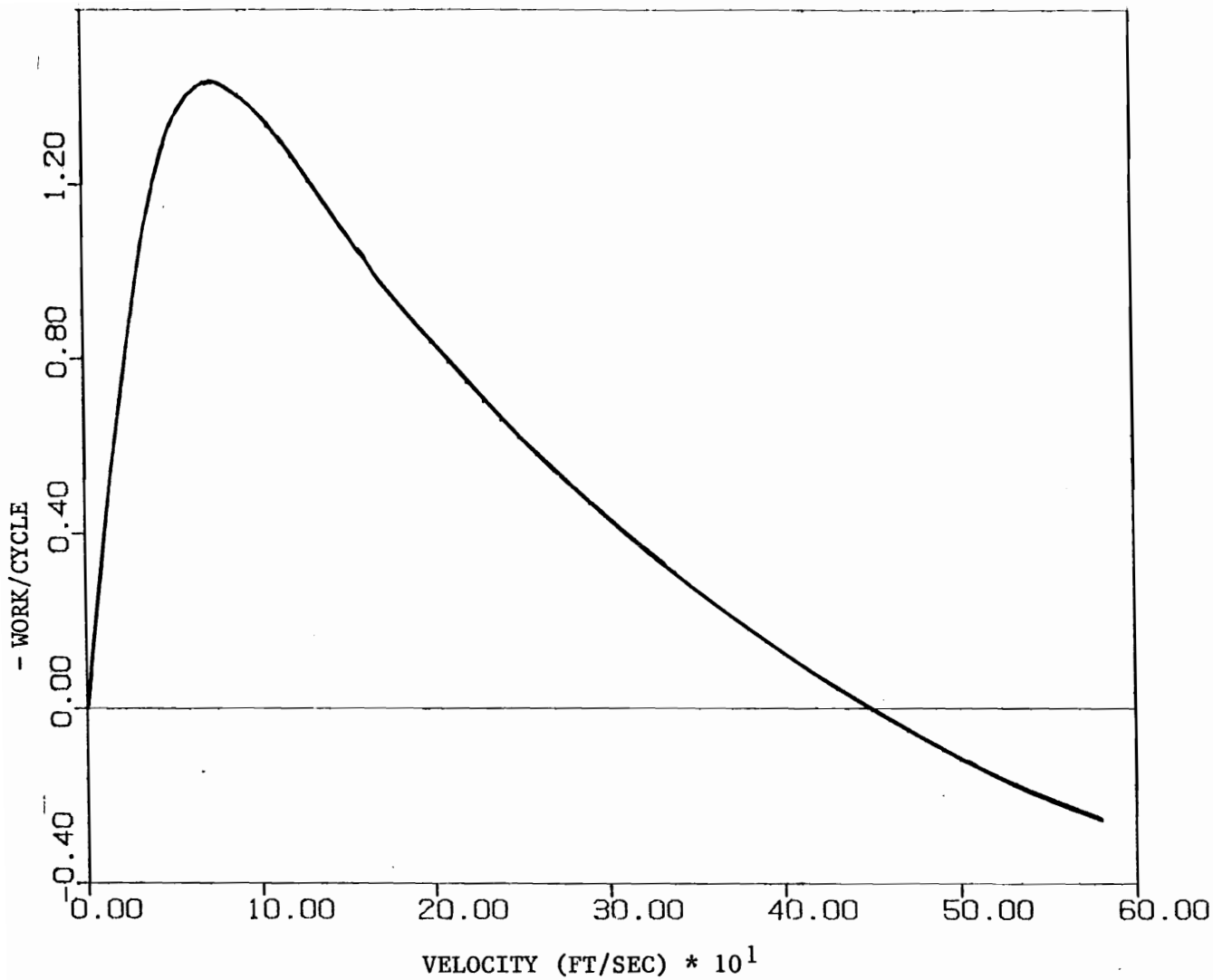

Figure 19. Work Per Cycle for the Synthesized Control Law, Zero Flap Inertia Case.

VITA

The author was born in Tulsa, Oklahoma on August 9, 1955. He received a Bachelor of Science degree in Aerospace Engineering from the University of Colorado in December, 1977. He entered the Aerospace and Ocean Engineering Department at Virginia Polytechnic Institute and State University in January, 1978.

Darrell L. York

ANALYSIS OF FLUTTER AND FLUTTER

SUPPRESSION VIA AN ENERGY METHOD

by

Darrell L. York

(ABSTRACT)

The use of an energy method for the synthesis of an active flutter-suppression control law is investigated. The derived control law is demonstrated on a two-dimensional wing having a single trailing-edge control surface. A procedure for control law implementation (i.e., forming the closed-loop system representation) is developed using the concepts of geometric theory and is illustrated for a simple two degree-of-freedom spring-mass system. The two-dimensional unsteady aerodynamic forces for oscillatory motion are taken from the literature. The aerodynamic forces in the time domain are found from a Fourier transform of the oscillatory aerodynamic forces. With the aid of a Wagner function approximation the unsteady aerodynamic forces are written in a standard state space form which is then combined with the mechanical equations of motion to yield the overall system state space representation. The results show that the flutter speed of an example airfoil can be increased significantly using the synthesized control law.